“Numerical Modelling of actin cytoskeleton”

A Seminar submitted in the partial fulfilment of the requirements for the award of the degree of

MASTER OF ENGINEERING

in

CIVIL ENGINERING

(STRUCTURES)

by

V Karthik
(800922012)

Under the guidance of

Dr. Abhijit Mukherjee

DEPARTMENT OF CIVIL ENGINEERING
THAPAR UNIVERSITY, PATIALA
2011

CERTIFICATE

This is to certify that the Thesis titled "**Numerical modelling of actin cytoskeleton**", being submitted by Mr. V Karthik, Roll No 800922012 in partial fulfilment for award of degree **Master of Engineering in Civil (Structures) at THAPAR UNIVERSITY, PATIALA,** is a bonafide work carried out by him under my guidance and supervision and that no part of this thesis has been submitted for the award of any other degree.

(Dr. Abhijit Mukherjee)
Director
Thapar University, Patiala
(Supervisor)

(Dr. Manoek Kumar)
Prof. & Head, CED
Thapar University, Patiala

(Dr. S.K.Mohapatra)
Dean Academic Affairs
Thapar University, Patiala

ACKNOWLEDGEMENT

I wish to affirm my earnest acknowledgement and indebtedness to **Dr. Abhijit Mukherjee**, Director, Thapar University, Patiala for his intuitive and meticulous guidance and perpetual inspiration. His blessings and motivation have always provided me a high inspiration.

I am heartily thankful to **Dr Shweta Goyal,** Assistant professor, Civil engineering department, **Dr. Haripada Bhunia**, Assistant Professor, Chemical engineering department and **Mr. Karun Verma**, Assistant Professor, Computer Science and engineering department for their support.

I would also like to thank all the staff members of **Civil Engineering Department** for their support and encouragement. The meaning of my life and work is incomplete without paying regards to my respected parents whose blessings and continuous encouragement have shown me the path to achieve my goals.

I owe my sincere thanks to **Mr. Abhilash A S**, Mechanical engineering department, National university of Singapore.

I am also thankful to the authors whose works I have consulted and quoted and my friends for being there throughout the whole time.

Last but not the least I would like to thank **Mr Nikhil Mohan** because a friend in need is a friend indeed and he has been of immense help throughout.

Above all, I pay my regards **Almighty** for his love and blessings.

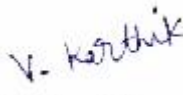

V Karthik

ABSTRACT

Over the last decade there has been a lot of interest in understanding the microscopic properties of network polymers because the networks of filamentous proteins play a crucial role in cell mechanics. These networks largely determine the viscoelastic response of cells. We study various model systems of cross-linked filaments in order to explore the connection between the topology under strain and the macroscopic response of cytoskeletal networks. We find that the behaviour of these networks is largely dependent on the random architecture and the cross linking density of the network. An account for the motility of the cells has also been included in the study by putting the topology under a predefined thermal field.

CONTENTS

LIST OF FIGURES

LIST OF TABLES

CHAPTER 1 INTRODUCTION

In the past decade, there has been rapid advancement in the field of engineering, technology, information sciences and medicine, as well in the growing trend to integrate such advances across multidisciplinary boundaries. This has produced spectacular progress in the study of mechanics and physics at the levels of individual cells and biomolecules. Improvements in computer hardware and software over the past decade has also facilitated in the development of such studies.

So far there has been a lot of research in determining the mechanical properties of Actin networks. But to determine these properties computationally everyone has identified certain parameters like cross link density L/l_c (Head et al., 2003) or line density (Onck et al., 2005) and modelled the networks keeping in mind these parameters. But at the core of all these lies assumptions about the deciding network parameters that would decide how the overall network would look like and this is where the basic difference lies between what has already been done and what we are trying to achieve.

Our work takes a totally different approach towards mechanical modeling of actin networks. We model the actin networks by using a simple micrograph of these biopolymers. Using micrographs as input we recreate the original network by converting the raster (original image) to vector and feeding this as an input to a designing software and getting back the original image in a vector form, thereby omitting any or all assumptions about the deciding network parameters. Thus the model so generated by such a process would yield a more realistic structure since it would not be a mere model but an actual network as seen in the micrograph.

To get a better understanding of what actin is and how it participates in the activities of a cell, a brief description of a cell is given as follows:

It is the smallest unit of life that is classified as a living thing, and is often called the building block of life (Bruce, 2002) The number of cells in the human body is literally astronomical, about three orders of magnitude more than the number of stars in the Milky way. Yet, for their immense number, the variety of cells is mucch smaller : only about 200 different cell types are represented in the collection of about 10^{14} cells that make up our bodies. The basic structural elements of most cells, however, are the same : fluid sheets enclose the cell and its compartments, while networks of filaments maintain the cell’s shape and help organize its contents (Boal, 2002).

The cytoplasm is a thick liquid residing between the cell membrane holding all the cell's internal sub-structures (called organelles), except for the nucleus. The cytoplasm has three major elements; the cytosol, organelles and inclusions. The cytoplasm also contains the protein filaments that make up the **cytoskeleton**, as well as soluble proteins and small structures such as ribosomes, proteasomes, and the mysterious vault complexes.(http://en.wikipedia.org/wiki/Cytoplasm)

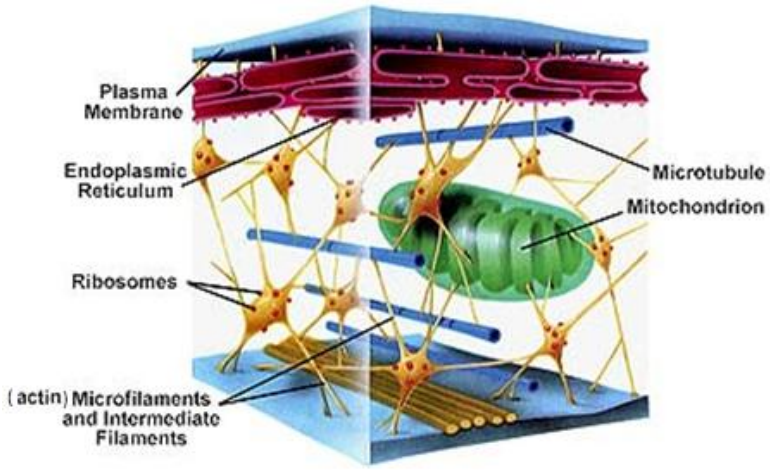

Fig 1.1 : Different parts of the cytoplasm (http://people.eku.edu/ritchisong/RITCHISO/301notes1.htm**)**

The mechanical properties of a cell are largely determined by its cytoskeleton (e.g., Hesketh and Prym, 1995; Howard, 2001; Boal, 2002), a self-organizing network of three primary protein filaments: microtubules, intermediate filaments, and actin filaments (microfilaments).

1.1 Actin

The protein **actin**, which forms one of the cell's principal filaments (microfilaments) , is found in organisms ranging from yeasts to humans. The elementary actin building block is the protein G-actin (G for globular), a single chain of approximately 375 amino acids having a molecular mass of 42,000 daltons. G–actin units can assemble into a long string called F-actin (F for Filamentous), which as illustrated in fig 1.2 has the superficial appearance of two strands forming a coil, although the strands are not, in fact, independantly stable. The filament has a width of about 7 nm and a mass per unit length of 16,000 daltons/nm (Boal , 2002).

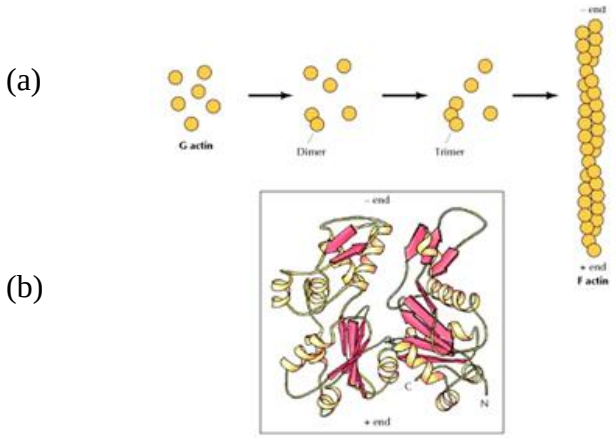

Fig 1.2 : (a) Actin monomers (G actin) polymerize to form actin filaments (F actin). The first step is the formation of dimers and trimers, which then grow by the addition of monomers to both ends. (b) Structure of an actin monomer (Cooper, 2000)

It is a major constituent of the cytoskeletal network that is an essential mechanical component in a variety of cellular processes, including motility and division (Lodish et al., 1999 and Kreis et al., 1999). There is broad experimental evidence from various methods that the actin cytoskeleton plays a predominant role in the elastic response or structural strength of cells (Tseng and Wirtz, 2001; Wang, 1998; Sato et al., 1990; Elson, 1988; Stossel, 1984). One simple method by which this has been shown is treating cells with actin depolymerizing drugs such as cytochalasin or latrunculin (Rotsch and Radmacher, 2000; Haga et al., 2000). These studies find that disrupting the actin network with drugs leads to a three-fold decrease in cell elasticity, while depolymerizing microtubules and intermediate filaments with appropriate agents does not have as significant an effect on the cell's structural strength. However, these cannot be used as differential or quantitative measurements since a depolymerized actin cytoskeleton disturbs the entire cell's structural integrity. Recent theoretical and in vitro work predicts the range that actin networks can contribute to the structural strength of cells (Gardel et al., 2004).

Actin filaments fall under the category of semi flexible filaments i.e., the filaments having Persistence length ≈ Contour Length. The Persistence length is the distance over which the filaments appear straight and the Contour length is its length at maximum physically possible extension. The other category of filaments are the flexible filaments (the filaments in which the Persistence Length << Contour Length) and the rigid filaments (the filaments in which Persistence Length >> Contour Length).

Actin filaments are characterized by both affine and non-affine deformations depending on the different concentration levels, molecular weight, etc. In an affine deformation as shown in figure 1.3 A, the small light green and dark green rectangles deforms in the same way the macroscopic deformation of the bigger rectangle which encompass both of them. Deformations are homogenous and elastic energy is primarily stored in the extension/contraction of filaments.

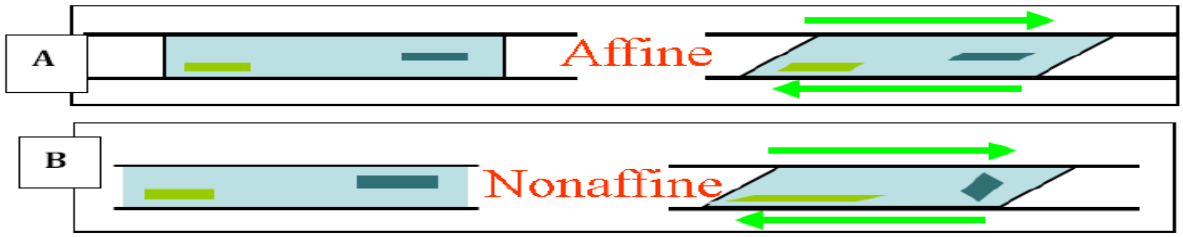

Figure 1.3 : Affine and non-affine deformations (Levine, 2005)

In a non-affine deformation as shown in figure 1.3 B, small light green and dark green rectangles deforms in different way than the macroscopic deformation of the bigger rectangle which encompass both of them. Deformations are heterogeneous and static shear modulus scales linearly with the bending modulus of the individual filaments (Levine, 2005).

1.2 Outline of the work

Chapter 1 – Introduction

This chapter gives a brief introduction of the work and explains what is actin.

Chapter 2 – Review of literature

This chapter gives the review of the literature's that have been referred and from where the gap between what has been done and what was needed to be done was understood.

Chapter 3 – Raster-Vector transformations

This chapter is basically divided into 2 phases. The first phase focuses on creating a two-dimensional network model of the different actin cytoskeleton's from the available electron micrographs and the second focuses on filtering the vector obtained to get a more refined structure and also to cut the time taken for analysis.

Chapter 4 – Behavior of actin topologies

This chapter focuses on the behavior of different actin topologies, where we first characterize different topologies and then find the RVE before discussing the mechanical response of the different actin topologies towards specified displacements.

Chapter 5 - Modelling the Actin cytoskeleton and cell motility

In this chapter a whole cell actin cytoskeleton has been modelled and an attempt has been made to describe cell's motility in terms of varying thermal field.

Chapter 6 - Conclusion and future work

This chapter contains all the conclusions and tries to give areas for future work.

Chapter 7 – References

In the last and final chapter, the references of all the literature from which guidance and help has been taken, are summarized.

CHAPTER 2 REVIEW OF LITERATURE

Over the past decade or so, a lot of time and effort has been spent on understanding the mechanical behavior of cells but still it remains a topic that is at best, loosely understood. Out of the vast amount work that has been done, a brief review of literature is being presented here :

Suresh S (2007) presents an overview of the rapidly expanding, nascent field of research that deals with the biomechanics and biophysics of cancer cells with some key observations on the biology of cancer cells and on the role of actin microfilaments, intermediate filaments and microtubule biopolymer cytoskeletal components in influencing cell mechanics, locomotion, differentiation and neoplastic transformation.

Onck et al., (2005) explored the strain stiffening of filamentous protein networks by means of a finite strain analysis of a 2-D network model of cross linked semi flexible filaments. They found that the stiffening is caused by a non-affine network rearrangement that governs the transition from a bending dominated response at small strains to a stretching dominated response at larger strains.

Figure 2.1 : Basic 2-D random network model of Actin (Onck et al., 2005)

He describes networks based on a non dimensionalised parameter $\bar{\rho}$, a parameter describing line density.

$$\rho = NL/W^2 \quad \ldots (1)$$

$$\bar{\rho} = \rho L \quad \ldots (2)$$

where, L = Length of each filament

N = number of filaments (assuming all filaments are of the same length)

W = width of square unit cell

Storm et al., (2005) developed a theory that accounts for the strain stiffening for a wide range of molecularly distinct gels. The theory made critical assumptions with regard to the network being homogenous, isotropic and that it would strain uniformly. This theory showed that the system of filaments invariably stiffen at low strains without requiring a specific architecture or multiple element with different intrinsic stiffness.

Yamazaki et al., (2005) did a review with focus on the migration of cancer cells and regulatory mechanism involving the actin cytoskeleton. They found that the inhibition of actin polymerization suppresses most types of cell migration.

Gardel et al., (2004) shows that the cross linked networks exhibit exceptional elastic behavior that reflects the mechanical properties of individual filaments. There are two distinct regimes of elasticity of which they talk about, one reflecting bending of single filaments and a second reflecting stretching of entropic fluctuations of filament length.

Head et al., (2003a) studied a model system of cross linked stiff filaments in order to explore the connection between the microstructure under strain and the macroscopic response of cytoskeletal networks. They found two distinct regimes as a function of cross link density and filament rigidity: one characterised by affine deformation and one by non-affine deformation and also characterised the cross over between the two.

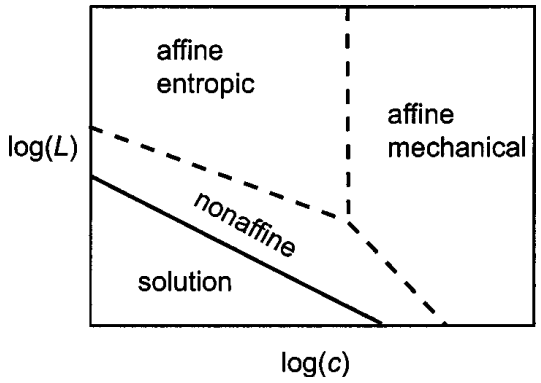

Figure 2.2 : A sketch of the expected diagram showing the various elastic regimes in terms of molecular weight L and concentration $c \sim 1/l_c$. (Head et al., 2003b)

Head et al., (2003b) performed numerical studies of the linear response of homogeneous and isotropic two-dimensional networks subjected to an applied strain at zero temperature. They found that the elastic moduli vanish for network densities at a rigidity percolation threshold. For higher densities, two regimes are observed: one in which the deformation is predominately affine and the filaments stretch and compress; and a second in which bending modes dominate.

He describes the density in terms of cross link density L/l_c.

L = length of each element

l_c = mean distance between cross links along a filament

so, $L/l_c - 1$= mean number of cross links per filament … (3)

Mackintosh et al., (1995) developed a model of cross linked gels of semi flexible biopolymers such as F-actin. In this model they explained a number of elastic properties of such networks in vitro including the concentration dependence of the storage modulus and yield strain.

Holmes et al., (1990) constructed the first atomic model of the F actin filaments. They found a unique orientation of the monomer with respect to the actin helix.

CHAPTER 3 RASTER-VECTOR TRANSFORMATIONS

Raster-Vector transformation is the process of converting a Raster into a Vector i.e., converting an image into editable format. It is necessary to covert a raster into a vector because all the software's of P-Δ analysis work with vector's i.e., entities are described spatially in terms of their Cartesian co-ordinates. Hence it is imperative to convert a raster to a vector so that it can be used in the software's of P-Δ analysis.

Raster-Vector transformation is used extensively in commercial and industrial applications and converts technical drawings, maps and other graphics from raster to vector formats providing easy archiving and quick access. Mapping and GIS data conversion are highly dependent on this application apart from architectural, construction, engineering, electrical and house plans.

In this chapter Raster-Vector transformation has been applied to a selected number of Actin topologies. As always the first step towards any such work is the validation. In the validation mode, Raster-Vector transformations were performed on different kinds of geometries. Since it yielded good and acceptable results, Raster-Vector transformation was then applied on selected Actin topologies. These different topologies are then scaled to the actual sizes by using scaling transformations.

The next step involves the vector refinement. This is done not only to make the mesh more refined but also to cut the cost of time taken for analysis. The vector refinement consists of three refinement process : Direction filter, intersection identifier and proximity filter. The direction filter works on the principle that if two or more consecutive line segments have almost the same slope, then these are invariably a single larger line segment instead of two consecutive smaller line segments. The intersection identifier is used to find out the intersection of the line segments. This is needed because the Raster-Vector transformation doesn't necessarily find the intersection of line segments but just converts the Raster into a vector. The Proximity filter as the name suggests filters out points in the proximity. This is introduced to further refine the output generated by the Raster-Vector transformation based on the distance of any point from the nearby points. This is essential because the Raster-Vector transformation generates unnecessary extra points which are in close proximity to each other which can be merged into a single point to make the mesh better and cut the time of analysis.

3.1 Raster

Raster (or bitmap) images are described by an array or map of bits within a rectangular grid of pixels or dots. When working with raster images, you edit pixels rather than objects or shapes. Raster images are the most common electronic medium for continuous tone images, such as photographs or scanned images because they can represent subtle gradations of shades and colors.

Raster Images can lose detail when scaled on-screen because they are resolution dependent, they contain a fixed number of pixels, and each pixel is assigned a specific location and color value. Raster images can look jagged if they are printed at too low a resolution because the size of each pixel is increased.

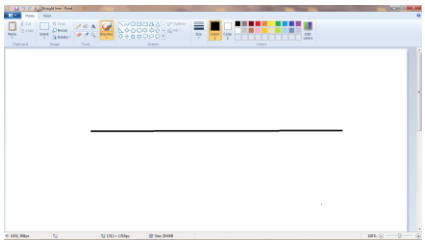

Fig 3.1 : A straight line drawn in MS Paint (Raster)

3.2 Vector

Vector images are described by lines, shapes, and other graphic image components stored in a format that incorporates geometric formulas for rendering the image elements. This means that you can move, resize, or change the color of a line without losing the quality of the graphic.

Vector graphics maintain crisp edges and lose no detail when resized, because they are resolution independent.

Vector of the above raster image :

POLYLINE	487 1049	1098 1050
281 1048	896 1049	END
486 1048	897 1050	

3.3 Validation of Raster-Vector transformations

Before applying the transformation on the actin topologies we must first confirm the adequacy of the process i.e., validation of raster-vector transformation needs to be carried out before using it on different actin topologies. In the validation mode we first drew many random lines and networks in MS Paint and then saved them as a JPEG file. Then these were converted to vectors with the help of image processing software. The output of the image processing software is a text file which contains co-ordinates of the image file. These co-ordinates / vectors were again fed as input into the design software (AutoCAD) to recreate models and then were compared to the original images. Three separate tests were conducted for this purpose and the results are as shown below :

- **Test 1**

First a simple line was created in MS paint and saved as JPEG file. It was then converted into a vector. This vector was then plotted to get the initial line back. The vector plotted identical line to the one that was initially created.

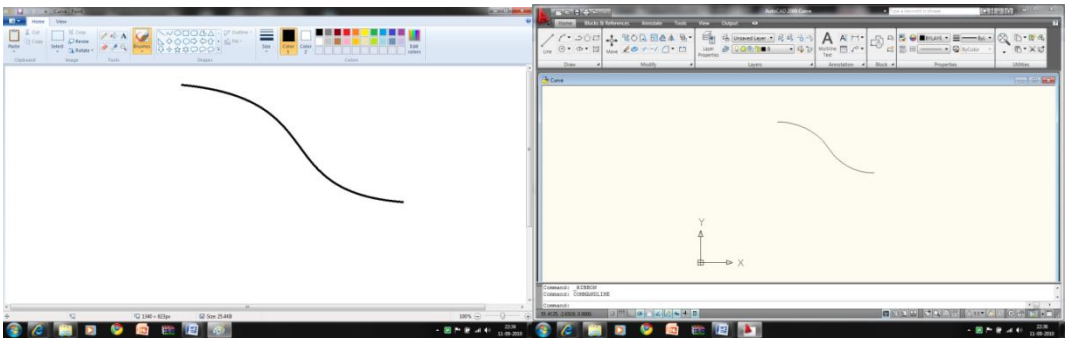

Fig 3.2 : A line drawn in MS Paint (Left) ; The vector plot in AutoCAD of the line drawn in MS Paint (Right)

The vector output file of the above figure :

POLYLINE	809 947	419 1207
870 942	760 957	388 1223
900 942	712 973	364 1230
901 943	661 998	351 1232
913 943	618 1026	323 1231
END	575 1061	318 1230
POLYLINE	501 1133	END
870 942	455 1179	

- **Test 2**

Then a hash was created and put through the same procedure. This also showed very good results as can be seen from the figures below. The two images side by side are identical to each other. This procedure is giving satisfactory results and hence was adopted for all future work.

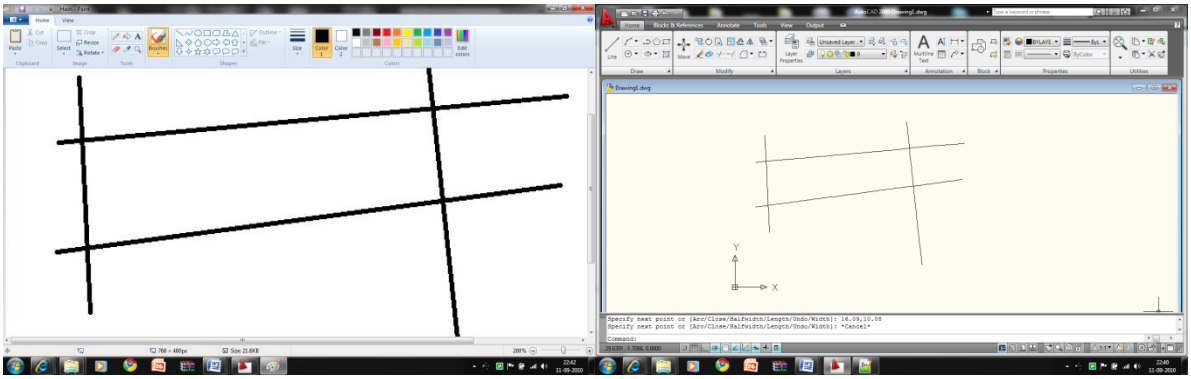

Fig 3.3 : A hash drawn in MS Paint (Left) ; The vector plot in AutoCAD of the hash drawn in MS Paint (Right)

The vector output file of the above figure :

```
POLYLINE
88      216
79      399
END
POLYLINE
88      216
91      148
END
POLYLINE
88      216
56      212
END
```

```
POLYLINE
88      216
472     267
598     284
END
POLYLINE
88      217
88      216
END
POLYLINE
472     267
461     373
```

```
454     435
END
POLYLINE
472     267
494     63
END
POLYLINE
82      332
76      332
75      331
65      331
64      330
```

```
58      330
END
POLYLINE
82      332
461     367
END
POLYLINE
463     367
605     380
END
```

- **Test 3**

Then a random set of lines was created and put through the same procedure. This also showed very good results as can be seen from the figures below. The two images side by side are identical to each other. This procedure is giving satisfactory results and hence was adopted for all future work.

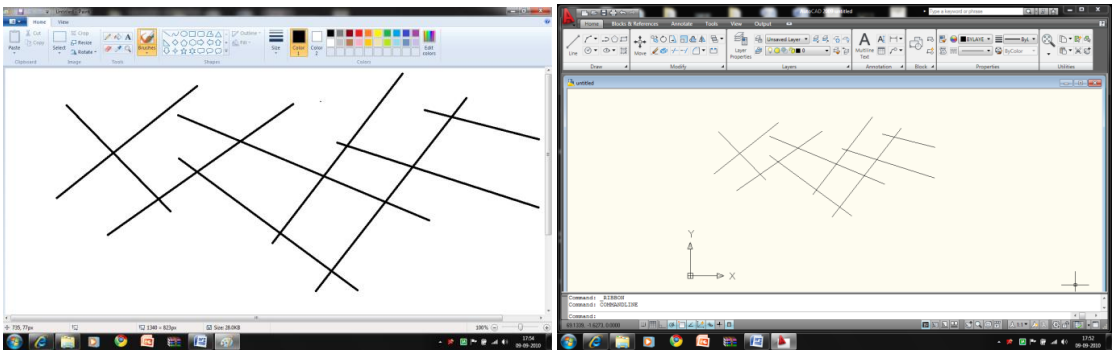

Fig 3.4 : A random set of lines drawn in MS Paint (Left) ; The vector plot in AutoCAD of the random set of lines drawn in MS Paint (Right)

The vector output file of the above figure :

POLYLINE	POLYLINE	218 1112	END	END
539 944	539 944	366 1250	POLYLINE	POLYLINE
538 947	523 922	END	338 977	612 1049
527 955	END	POLYLINE	415 1047	614 1049
418 1047	POLYLINE	336 977	END	744 981
414 1048	539 946	338 977	POLYLINE	747 981
374 1083	612 1048	347 966	415 1047	747 978
364 1091	612 1050	END	415 1048	664 842
END	493 1111	POLYLINE	END	666 839
POLYLINE	494 1116	336 977	POLYLINE	732 784
539 944	597 1207	274 921	418 1047	END
540 944	END	END	418 1046	POLYLINE
663 841	POLYLINE	POLYLINE	END	614 1049
637 798	539 946	336 977	POLYLINE	614 1048
END	538 946	335 978	418 1047	END
POLYLINE	END	END	460 1086	POLYLINE
539 944	POLYLINE	POLYLINE	488 1111	614 1049
540 943	336 977	338 977	486 1114	640 1087
END	218 1106	338 976	369 1175	671 1132

671 1135	804 1071	END	POLYLINE	783 1289
657 1138	750 983	POLYLINE	488 1112	END
END	750 978	215 1109	493 1112	POLYLINE
POLYLINE	828 938	216 1109	END	880 1198
815 1091	END	217 1108	POLYLINE	884 1198
675 1133	POLYLINE	217 1109	488 1112	1050 1150
671 1134	818 1091	END	487 1113	END
END	824 1104	POLYLINE	END	POLYLINE
POLYLINE	880 1196	215 1109	POLYLINE	884 1198
815 1091	880 1199	150 1048	493 1112	886 1205
819 1091	830 1213	END	494 1111	913 1249
1037 1026	END	POLYLINE	END	END
END	POLYLINE	215 1109	POLYLINE	
POLYLINE	215 1109	214 1110	675 1134	
815 1091	167 1162	END	681 1145	

3.4 Vectorization of Actin topologies

Since the validation mode yielded good and acceptable results, the process was deemed fit to be applied to different actin topologies. Out of a number of actin topologies reviewed, only 3 were chosen in the end and are presented in this report. After the process was validated, this process was applied on many different Actin topologies out of which we carefully choose three different Actin topologies which will be presented in this report. These three were selected because each one of them showed a distinct characteristic i.e., Actin topology 1 was predominantly a shear case; Actin topology 2 was predominant in y and Actin topology 3 predominant in x (refer Table : 4.1). These topologies were then converted into vectors.

3.4.1 Actin topology 1

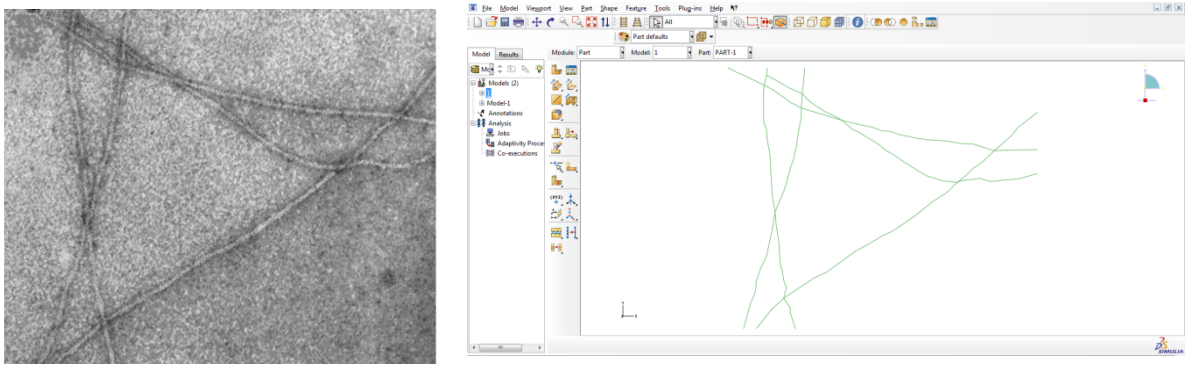

(a) (b)

Fig 3.5 : (a) Actin formed from CaATP–G actin in 0.1 M KCl (Rakoczy et al, 2009) (b) Vector image of actin formed from CaATP–G actin in 0.1 M KCl

If we look closely at the above figure you will see that the number of filaments that are aligned vertical and the number of filaments that are aligned horizontal are almost same. This fact is also substantiated by the direction cosines of this Actin topology. (refer Table 4.1) This network is neither predominant in x nor predominant in y but a case of predominance in shear

3.4.2 Actin topology 2

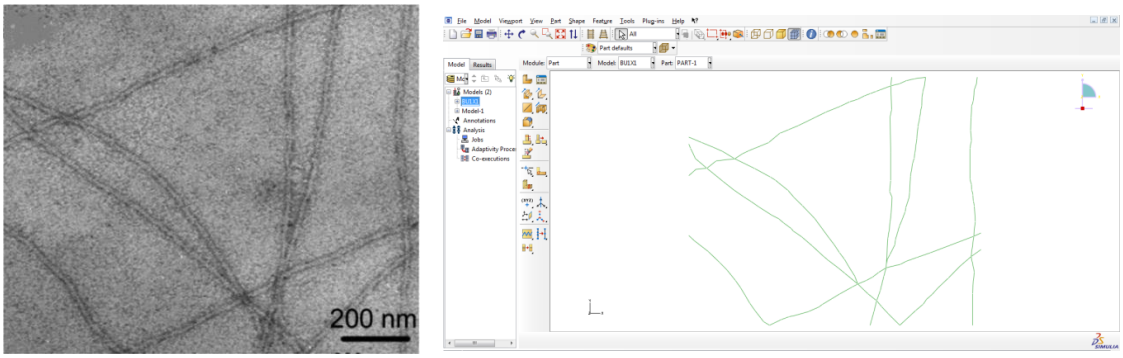

(a) (b)

Fig 3.6 : (a) Actin formed from MgATP-Gactins in 0.1 M KCl (Rakoczy et al, 2009) (b) Vector image of actin formed from MgATP-Gactins in 0.1 M KCl

A careful observation of the above figure would reveal that the orientation of the network is more towards y than x. This fact is also substantiated by the direction cosines of this Actin topology. (refer Table 4.1)

3.4.3 Actin topology 3

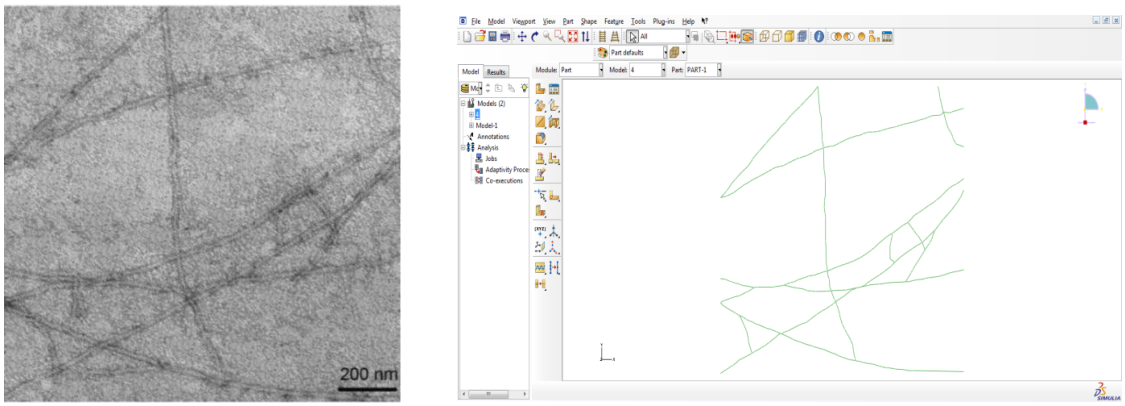

(a) (b)

Fig 3.7 : (a) F-actin filaments assembled from MgADP-G-actin in the presence of 0.1 M KCl (Rakoczy et al, 2009)
(b) Vector image of F-actin filaments assembled from MgADP-G-actin in the presence of 0.1 M KCl

The above figure on close observation reveals that the orientation of the networks is essentially towards x. This fact is also substantiated by the direction cosines of this Actin topology. (refer Table 4.1)

3.5 Scaling transformations

These vectors were then scaled to the actual dimensions by using a scaling function:

$$\bar{x} = S_x * x \quad \ldots (4)$$

$$\bar{y} = S_y * y \quad \ldots (5)$$

where,

S_x and S_y are scaling factors = (Actual dimension / Raster-vector transformation dimension)

x and y are the initial co-ordinates from the raster-vector transformation

$\bar{x}$ and $\bar{y}$ are the co-ordinates corresponding to the actual dimensions.

3.6 Vector Refinement

After the rasters are converted into vectors, the next step is to refine the vectors. This is done because the vectors generated by the raster-vector transformation usually have a very coarse data i.e., (a) the data could contain points / line segments which are factitious; (b) the output vector doesn't necessarily have a node at the intersection; (c) the data could contain points / line segments which can be omitted without changing the overall geometry of the structure. This not only leads to a more refined structure but also reduces the overall calculation time without affecting the overall geometry and the final results. This is achieved by applying :

1. Direction filter
2. Intersection identifier
3. Proximity filter

Before the direction filters are explained a few definitions are elaborated below :

Let be a point **p** with the Cartesian co-ordinates (x,y) be denoted as follows

$$\mathbf{p} = (x,y) \quad \ldots (6)$$

The **Distance** function calculates the Cartesian distance between two points:

$$\mathbf{Distance}(p_1,p_2) = \sqrt{(x_1-x_2)^2+(y_1-y_2)^2} \quad \ldots (7)$$

where $p_1 = (x_1,y_1)$

and $p_2 = (x_2,y_2)$

Let a line segment **L** be represented by an ordered pair consisting of its starting and ending points:

$$\mathbf{L} = (p_1,p_2) \quad \ldots (8)$$

The **Slope** function returns the slope of the given line segment:

$$\mathbf{Slope}(L) = \frac{(y_2-y_1)}{(x_2-x_1)} \quad \ldots (9)$$

where $p_1 = (x_1,y_1)$

and $p_2 = (x_2,y_2)$

Let **C** be a curve defined by the n consecutive points $p_1, p_2, \ldots, p_n$ making n-1 line segments :

$$\mathbf{C} = \langle p_1,p_2,\ldots,p_n\rangle \quad \ldots (10)$$

The **Line segments** function returns the line segments that make up a curve. So, for the above curve,

$$\boldsymbol{LineSegments}(C) = \langle (p_1,p_2),(p_2,p_3),\ldots,(p_{n-1},p_n)\rangle \quad \ldots (11)$$

The **Pairwise** function returns a set containing every possible pairwise combination of its elements. For example, if $X = (1,2,3,4)$,

$$\boldsymbol{Pairwise}(X) = \{(1,2),(1,3),(1,4),(2,3),(2,4),(3,4)\} \quad \ldots (12)$$

3.6.1 Direction Filter

The raster-vector transformation at times creates connected points / line segments that are essentially part of a curve with very large radius like the one shown in the fig 3.8. It can be seen that the curve has connected consecutive line segments that are separated by only a minor difference in slope. Hence the middle nodes can be deleted and the extreme nodes can be joined to make a smoother curve (in this this case a smoother set of line segments). The direction filter merges consecutive line segments within a curve if the difference in slope of consecutive line segments falls within the specified value. This is essentially a curve fitting or curve smoothing operation done on line segments.

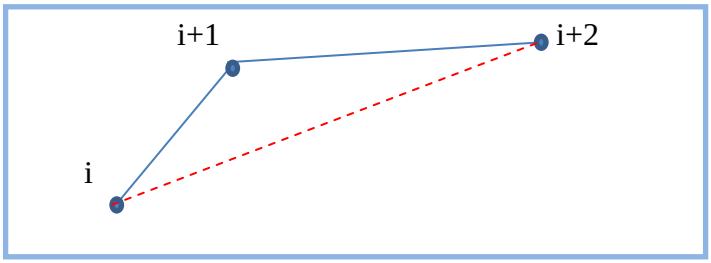

Fig 3.8 : The dotted line shows the line segment after the direction filter

The **Merge** function determines whether if it is within limits to merge two consecutive line segments of a curve into one.

$$\boldsymbol{Merge}(p_1,p_2,p_3) = \begin{cases} True, & if\ |Slope(p_1,p_2) - Slope(p_1,p_3)| \leq M \\ False, & \dots \quad Otherwise \end{cases} \quad \dots (13)$$

Start at point $i = 1$. If $\boldsymbol{Merge}(p_i,p_{i+1},p_{i+2})$ is True, delete point $i + 1$ and retest at point i. Otherwise, move to point $i + 1$. Continue until $i + 2 = n$, where n is the number of points that make up the curve.

3.6.2 Intersection identifier

The raster-vector transformation doesn't have any specific provisions for creating a node at the intersection and hence an intersection identifier is added externally to find out and add nodes at the intersections. This is done because the intersections are a very important part of the analysis as they are the physical connection between the whole network. The intersection identifier finds out the intersection of curves of line segments assuming that no line segment of a curve intersects any other line segment of the same curve.

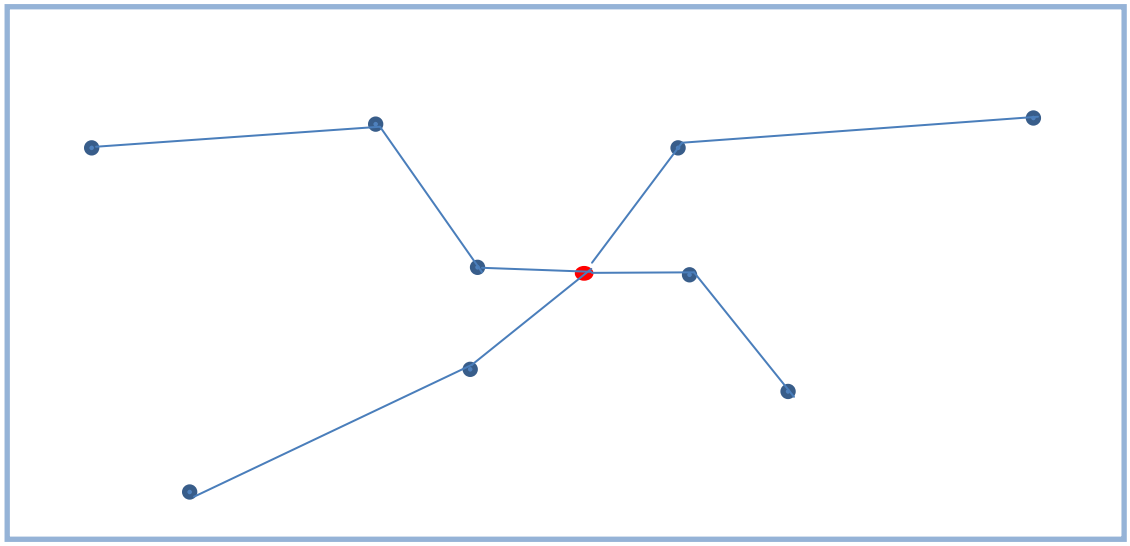

Fig 3.9 : Intersection identifier

The **Intersect** function returns the intersection point of two line segments if it exists:

$$\boldsymbol{Intersect}\big((p_1,p_2),(p_3,p_4)\big) = p' = \left(\frac{\begin{vmatrix} \begin{vmatrix} x1 & y1 \\ x2 & y2 \end{vmatrix} & \begin{vmatrix} x1 & 1 \\ x2 & 1 \end{vmatrix} \\ \begin{vmatrix} x3 & y3 \\ x4 & y4 \end{vmatrix} & \begin{vmatrix} x3 & 1 \\ x4 & 1 \end{vmatrix} \end{vmatrix}}{\begin{vmatrix} \begin{vmatrix} x1 & 1 \\ x2 & 1 \end{vmatrix} & \begin{vmatrix} y1 & 1 \\ y2 & 1 \end{vmatrix} \\ \begin{vmatrix} x3 & 1 \\ x4 & 1 \end{vmatrix} & \begin{vmatrix} y3 & 1 \\ y4 & 1 \end{vmatrix} \end{vmatrix}}, \frac{\begin{vmatrix} \begin{vmatrix} x1 & y1 \\ x2 & y2 \end{vmatrix} & \begin{vmatrix} y1 & 1 \\ y2 & 1 \end{vmatrix} \\ \begin{vmatrix} x3 & y3 \\ x4 & y4 \end{vmatrix} & \begin{vmatrix} y3 & 1 \\ y4 & 1 \end{vmatrix} \end{vmatrix}}{\begin{vmatrix} \begin{vmatrix} x1 & 1 \\ x2 & 1 \end{vmatrix} & \begin{vmatrix} y1 & 1 \\ y2 & 1 \end{vmatrix} \\ \begin{vmatrix} x3 & 1 \\ x4 & 1 \end{vmatrix} & \begin{vmatrix} y3 & 1 \\ y4 & 1 \end{vmatrix} \end{vmatrix}} \right)$$

… (14)

if $min(x_1,x_2), min(x_3,x_4) \leq x' \leq max(x_1,x_2), max(x_3,x_4)$

and $\min(y_1,y_2), \min(y_3,y_4) \leq y' \leq \max(y_1,y_2), \max(y_3,y_4)$

None, otherwise

where $p_1 = (x_1,y_1)$,

$p_2 = (x_2,y_2)$,

$p_3 = (x_3,y_3)$,

$p_4 = (x_4,y_4)$,

and $p' = (x',y')$

Let C denote the set of curves that make up the mesh. The following pseudo code illustrates how intersections between curves are determined:

For C_1 & C_2 in Pairwise(C)

    For l_1 & l_2 in LineSegments(C_1) × LineSegments(C_2)

        If Intersect(l_1, l_2), Add point to mesh

3.6.3 Proximity filter

The raster-vector transformation sometimes creates a cluster of points that are very close to each other like the one shown in the fig. 3.10. The proximity filter merges points that are close to each other i.e., any or all points that fall within the prescribed distance are all merged into one single point which has the mean co-ordinates of the cluster.

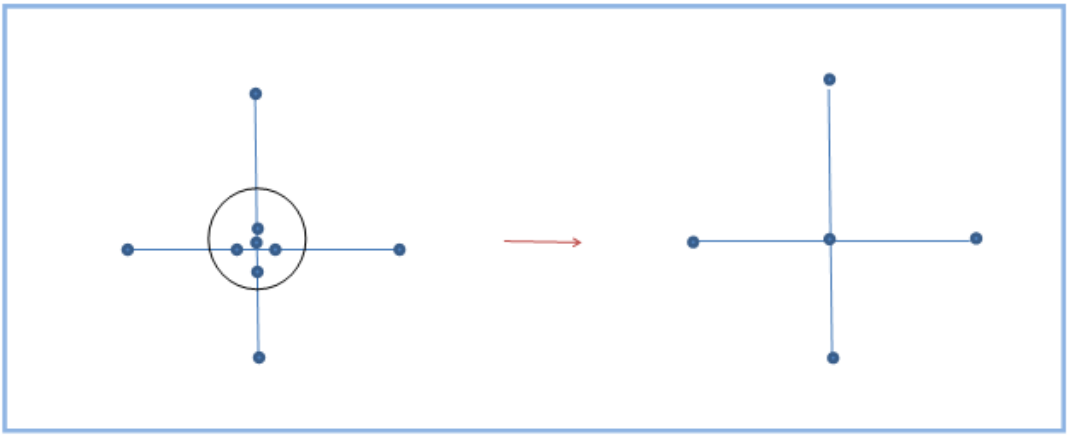

Fig 3.10 : Proximity filter

This filter partitions the set of points in the mesh into subsets where the distance between the points within a subset is less than or equal to the specified value and replaces points within a subset with the average value of that particular subset.

Let **P** be the set of points that form the mesh.

$$\mathbf{P} = (p_1, p_2, \dots, p_n) \quad \dots (15)$$

Partition **P** into subsets $P_1, P_2, \dots, P_m$ such that $\forall\ P_i$,

$$\text{Distance}(p_j, p_k) \leq D \quad \dots (16)$$

$$\forall\ 1 \leq j, k \leq n$$

For all P_i,

$$\text{Let } p_i^* = \frac{1}{n_i} \sum_{j=1}^{n_i} P_{ij} \quad \dots (17)$$

$$\text{where } n_1 = n(P_i)$$

Replace all points $p \in P_i$ with p_i^* in P.

3.6.4 Statistics

Table 3.1 Statistics of vector refinement

Refinement	Actin Topology 1		Actin Topology 2		Actin Topology 3	
	Nodes	Elements	Nodes	Elements	Nodes	Elements
Initial Vector	473	440	582	542	1176	1120
After Direction filter	434	399	519	477	1051	991
After Intersection identifier	433	399	517	477	1050	991
After Proximity filter	114	118	165	170	360	371

For the refinement using the Direction filter was used with a max value of 0.04. Exceeding this critical value distorts the whole networks. It starts eating up data i.e., far too many points are merged and the final structure so created bears no resemblance to the original image.

In case of the Proximity filter, the max value used is 12 units. Exceeding this critical value will lead to loss of data and form. For example, if we keep on increasing this value and get to the value equal to the size of the mesh, then only one point will remain in the mesh. Hence this filter is to be used with good judgement.

It can be seen from the above statistics that the direction filter is the one that filters out the most points as compared to any other filter and hence is the more effective of the two filters.

The figures 3.11 to 3.14 show topology 1 from the initial vector stage to the vector after the proximity filter.

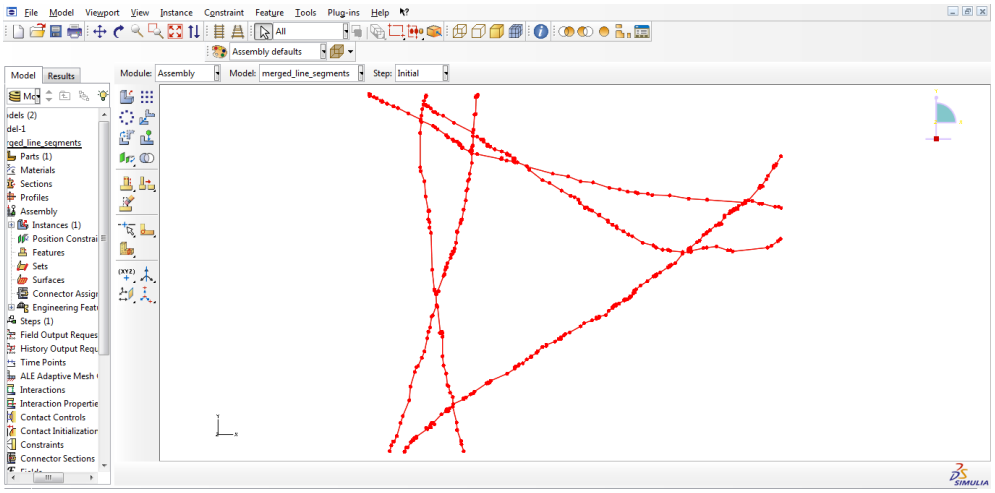

Fig 3.11 : Initial Vector of actin topology 1

The figure 3.11 shows the actin topology 1 right after the raster-vector transformation i.e., the initial vector. This vector is then refined using the refinement as discussed earlier.

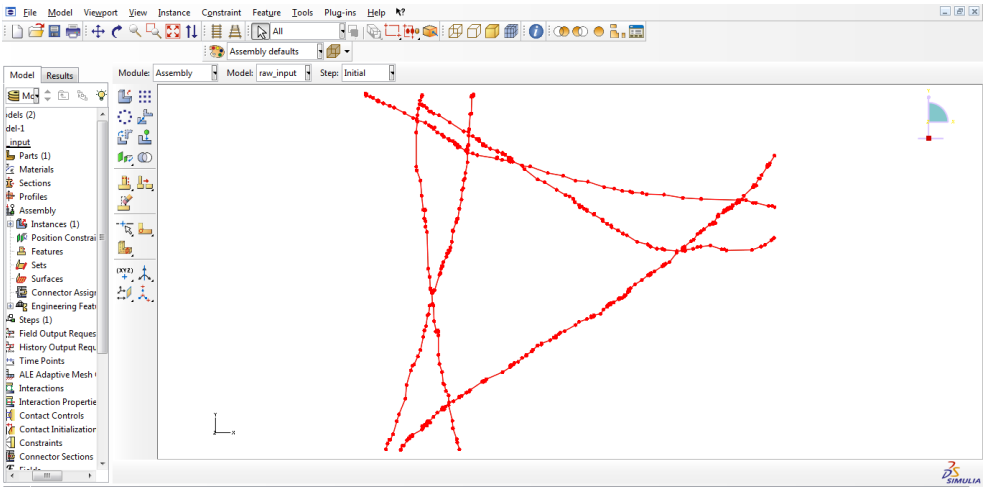

Fig 3.12 : Actin topology 1 after direction filter

The figure 3.12 shows the actin topology 1 after the direction filter. The number of points in the mesh is only slightly reduced as compared to the initial vector as can be seen from the figure above. This fact is not that clearly visible as only about 9% of nodes are reduced.

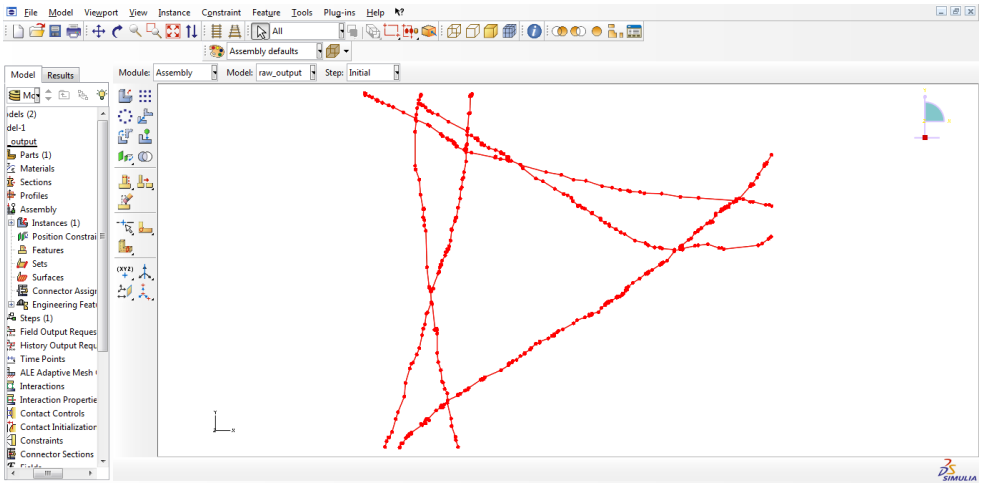

Fig 3.13 : Actin topology 1 after intersection identifier

The figure 3.13 shows the actin topology 1 after the application of the intersection identifier. There is only little change in the mesh as compared to the earlier one as only the missing intersections are added.

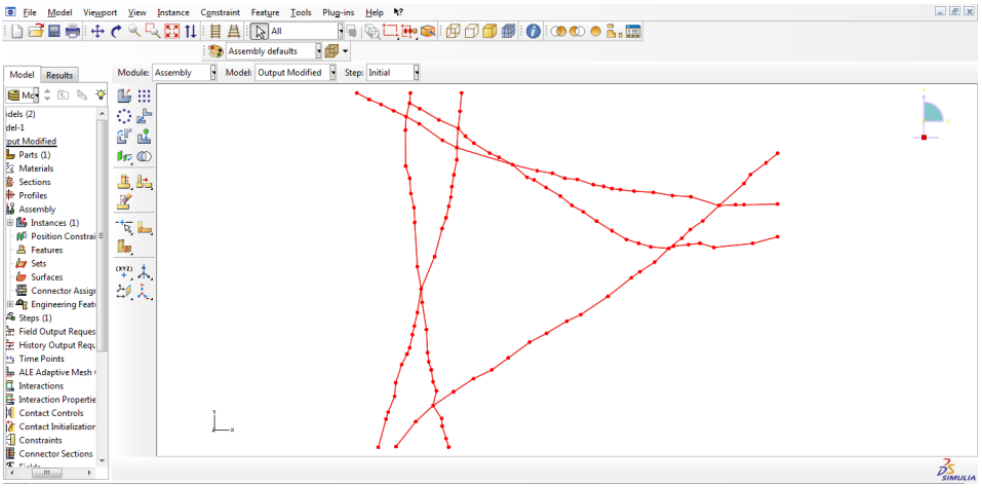

Fig 3.14 : Actin topology 1 after proximity filter

The figure 3.14 shows the actin topology 1 after the application of proximity filter. As can be seen from the above figure, this is the more effective filter as it refines the mesh the most out of the two filters. Approximately 74% of nodes are reduced by this filter but the overall geometry remains almost unaltered which is clearly visible in the above figure.

CHAPTER 4 BEHAVIOR OF ACTIN TOPOLOGIES

One major similarity that is found in many of the papers is that the actin topologies show hard spring behaviour. The figure below shows three curves showing (1) Hard spring behaviour (2) Linear elastic behaviour (3) Soft spring behaviour. The network polymers usually show the hard spring behaviour (Strain hardening) owing to its network structure.

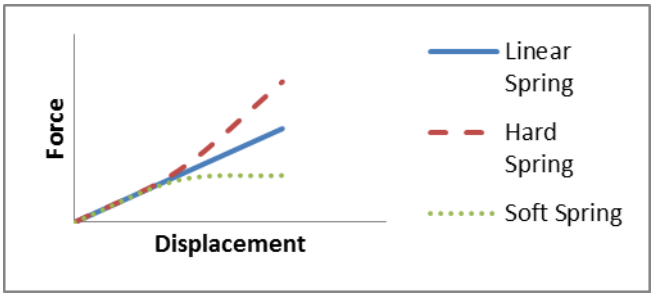

Figure 4.1 : Force displacement relation of a Hard Spring, Linear Spring and Soft Spring. (Paz, 2004)

The above figure shows 3 curves depicting hard spring, linear spring and soft spring behaviours. In a "hard spring" the force required to produce a given displacement becomes increasingly greater as the spring is deformed. In a "linear spring" the deformation is directly proportional to the force and the graphical representation of its characteristic is a straight line. In a "soft spring" the incremental force required to produce additional deformation decreases as the spring deformation increases (Paz, 2004).

The hard spring behaviour is caused because of the cross linking of the network. The effect of cross links can be explained as follows :

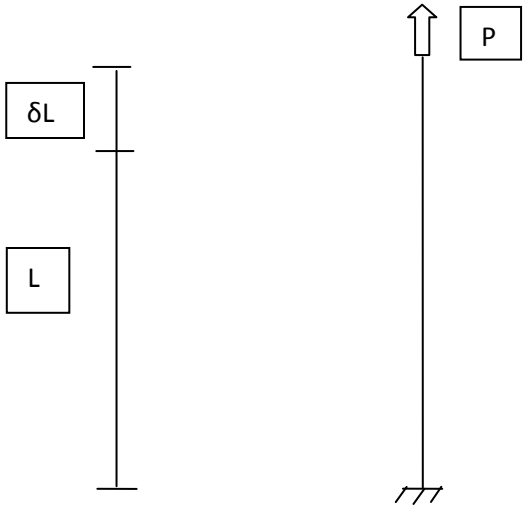

Figure 4.2 : Axial deformation of a single filament subjected to a load P

The figure 4.2, shows an element that is fixed at its base. A load P is applied at the top causing the element to elongate. If no other element is present in the network then this element would elongate by a distance δL.

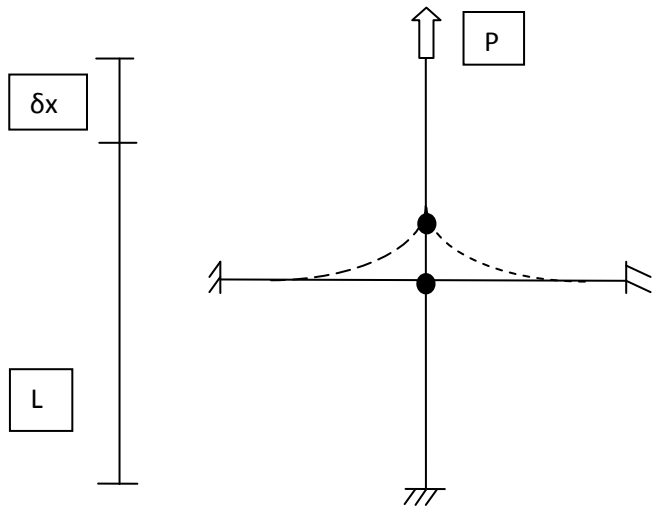

Figure 4.3 : Axial deformation of a network subjected to a load P

Now say another element is present as shown in figure 4.3. After the application of the same load P, the filament gets stretched and the horizontal members no longer remain horizontal and get pulled with the vertical member as shown by dotted line in fig 4.3. As the angle keeps on increasing, the horizontal members start to contribute more and more. Because if we resolve the force in the members, initially since the horizontal members is at 0 inclination it has no component in the vertical axis but as the member is pulled its inclination changes from 0 to a finite value depending upon the force. At any given state apart from the initial one it would have a component in the vertical axis as well and hence will share the force coming on the vertical member leading to a hard spring behaviour. In other words, $\delta x < \delta L$ i.e. hard spring behaviour is induced due to cross linking of filaments because as the filament gets stretched, the horizontal members no longer remains horizontal and get pulled with the vertical member as shown in fig 4.3, and participates in sharing the load.

The software of choice for analysis in our case is Abaqus. The vector from the Raster-Vector transformation after undergoing the vector refinement is fed as input to Abaqus for analysis. In this chapter after the characterization of actin topologies, convergence study is carried out to find the RVE that would be satisfactory. After that is established , the comparisons are made between the behaviour of different actin topologies.

4.1 Characterization of Actin topologies

The different actin topologies were characterized on the basis of their direction cosines. The direction cosines of a vector are merely the cosines of the angles that the vector makes with the x and y axes, respectively. We label these angles α (angle with the x axis) and β (angle with the y axis).

Let x' and y' be the projection of the filaments on the x and y axes respectively. Then,

$$x' = \frac{\sum x2 - x1}{L} \; and \; y' = \frac{\sum y2 - y1}{L} \qquad \ldots (18)$$

where, L = Total length of the filaments

$$= \sum \sqrt{(x2 - x1)^2 + (y2 - y1)^2}$$

Hence the direction cosines are given by :

$$\alpha = \frac{(x')^2}{\sqrt{((x')^2 + (y')^2)}} \; and \; \beta = \frac{(y')^2}{\sqrt{((x')^2 + (y')^2)}} \qquad \ldots (19)$$

Table 4.1 : Direction cosines of different Actin topologies

Actin topology	Direction cosine	
	α (x – direction)	β (y – direction)
1	0.714818257	0.699310274
2	0.637900558	0.770118742
3	0.838215965	0.545338423

From the above table we can deduce that :

- In Actin topology 1, we can see that the difference in the values of the direction cosines is very less. This would result in an overall structure that would be predominantly a shear case.
- In Actin topology 2, the difference is higher and β has a high value. This would result in an overall structure that is predominant in y.
- In Actin topology 3, the difference is the highest and the value of α is much larger value. This would result in an overall structure that is predominant in x.

4.2 Convergence study

The convergence of the results was tested by applying a specified displacement in x – direction, a specified displacement in y – direction and a specified shear deformation in Abaqus. Using repeating units of a unit cell, larger cells were created using tiling were put under the above specified conditions.

Table 4.2 Network parameters used

Parameter	Value
Diameter of each filament	7 nm (Gardel et al., 2004)
Elastic modulus of each filament	1.8 GPa (Kojima et al., 1994)
Element used	Beam
Poisson's ratio for each filament	0

(a) Actin topology 1

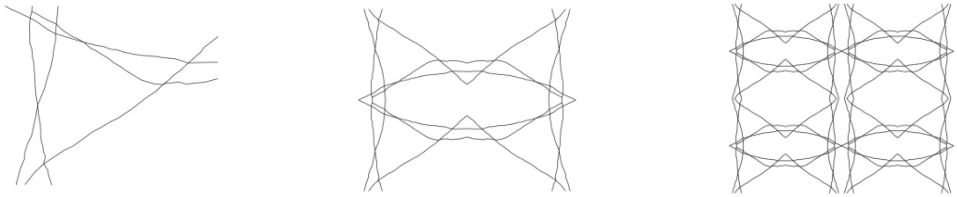

(1 x 1 RVE) (2 x 2 RVE) (4 x 4 RVE)

(b) Actin topology 2

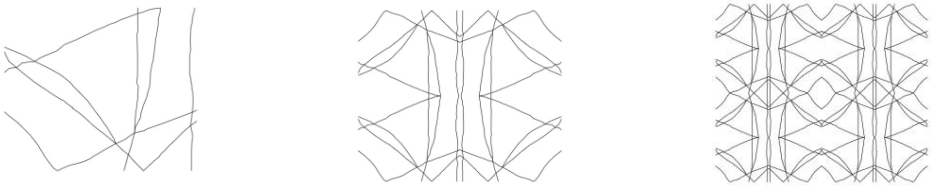

(1 x 1 RVE) (2 x 2 RVE) (4 x 4 RVE)

(c) Actin topology 3

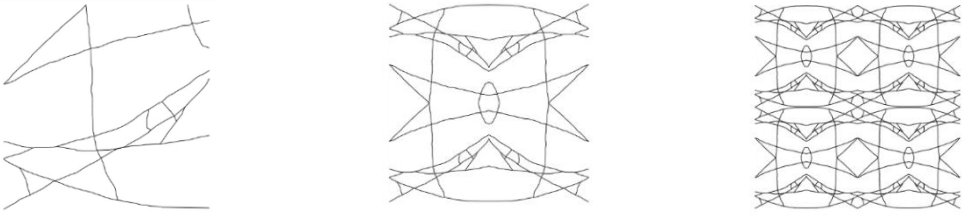

(1 x 1 RVE) (2 x 2 RVE) (4 x 4 RVE)

Fig 4.4 : 1 x 1, 2 x 2 and 4 x 4 RVE of (a) Actin topology 1 (b) Actin topology 2 (c) Actin topology 3

4.2.1 Specified displacement in x – direction

To test the convergence, a specified displacement was given in x – direction and the resulting stress v/s strain graph was plotted for 1 x 1, 2 x 2 and 4 x 4 RVE.

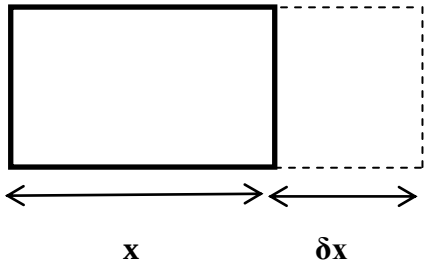

Fig 4.5 : Schematic diagram showing specified displacement in x - direction

4.2.1.1 Actin topology 1

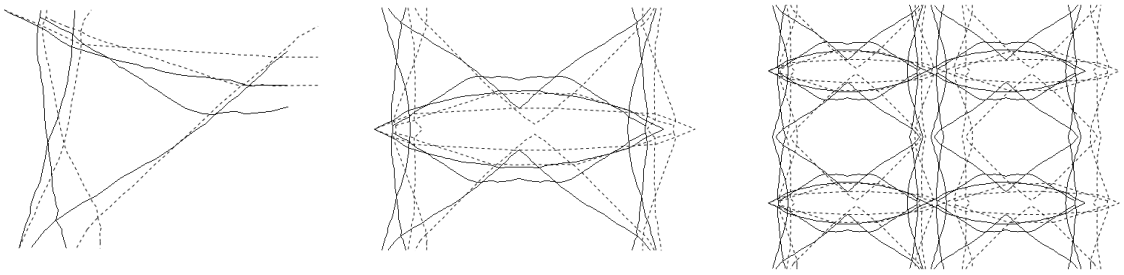

(a) (b) (c)

(d)

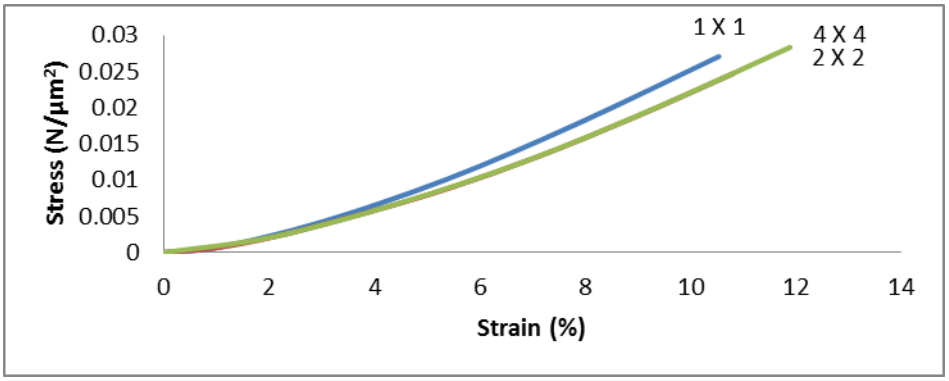

Fig 4.6 : (a) 1 x 1 RVE subjected to a specified displacement (b) 2 x 2 RVE subjected to a specified displacement (c) 4 x 4 RVE subjected to a specified displacement (d) Stress v/s Strain graph of Actin topology 1 for a specified displacement in x – direction.

From the above figure it can be seen that the 2 x 2 and 4 x 4 RVE's are overlapping each other. This shows that the model converges as we move from 1 x 1 to 2 x 2 and then to 4 x 4.

4.2.1.2 Actin topology 2

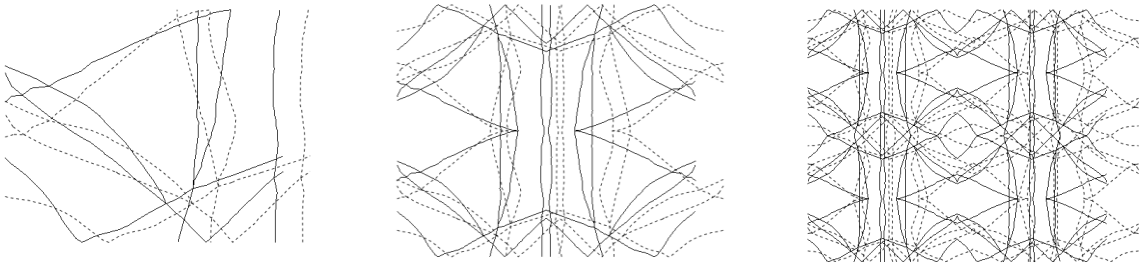

(a) (b) (c)

(d)

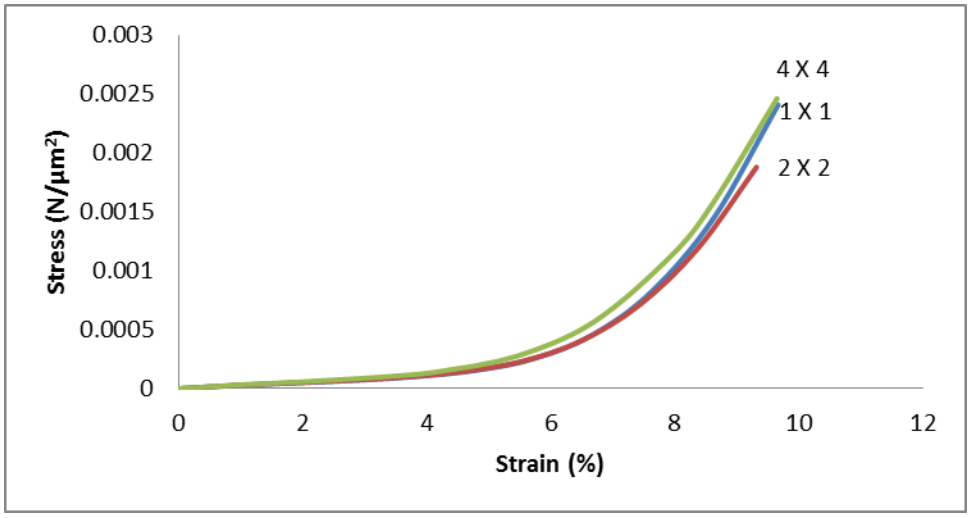

Fig 4.7 : (a) 1 x 1 RVE subjected to a specified displacement (b) 2 x 2 RVE subjected to a specified displacement (c) 4 x 4 RVE subjected to a specified displacement (d) Stress v/s Strain graph of Actin topology 2 for a specified displacement in x – direction.

The above graph does not show a proper convergence. The possible reason for it could be the lack of points on the right edge to pull the network from. For example, in fig 4.7 (a), on the right edge there are only 2 closely spaced points available to apply the specified displacement in x-direction which may be the cause for the deviation.

4.2.1.3 Actin topology 3

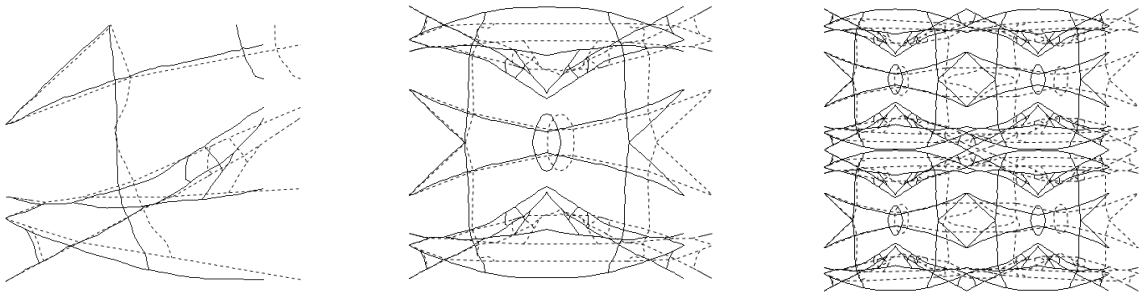

(a) (b) (c)

(d)

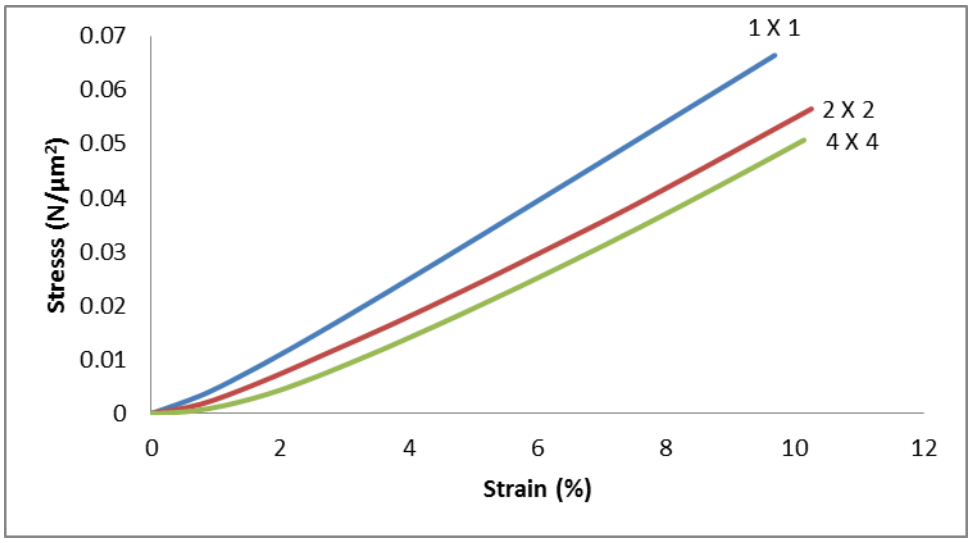

Fig 4.8 : (a) 1 x 1 RVE subjected to a specified displacement (b) 2 x 2 RVE subjected to a specified displacement (c) 4 x 4 RVE subjected to a specified displacement (d) Stress v/s Strain graph of Actin topology 3 for a specified displacement in x – direction.

It can be seen from the above graph that as we move from 1 x1 to 2 x 2 and then from 2 x 2 to 4 x 4, the difference between the two consecutive RVE's is reducing. Hence it can be inferred that the graph is converging.

4.2.2 Specified displacement in y – direction

To test the convergence, a specified displacement was given in y – direction and the resulting stress v/s strain graph was plotted for 1 x 1, 2 x 2 and 4 x 4 RVE.

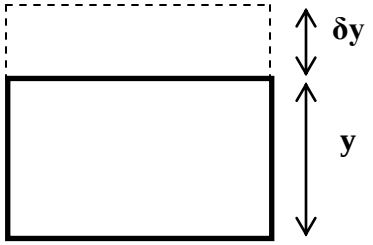

Fig 4.9 : Schematic diagram showing specified displacement in y - direction

4.2.2.1 Actin topology 1

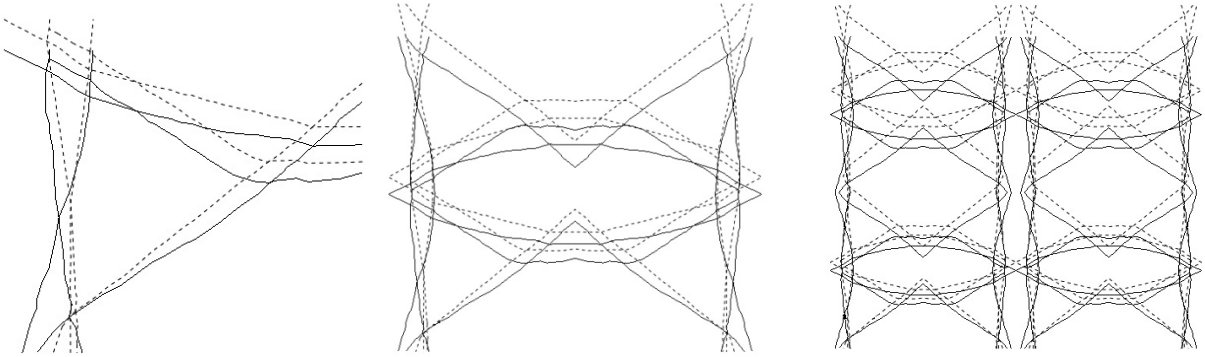

(a) (b) (c)

(d)

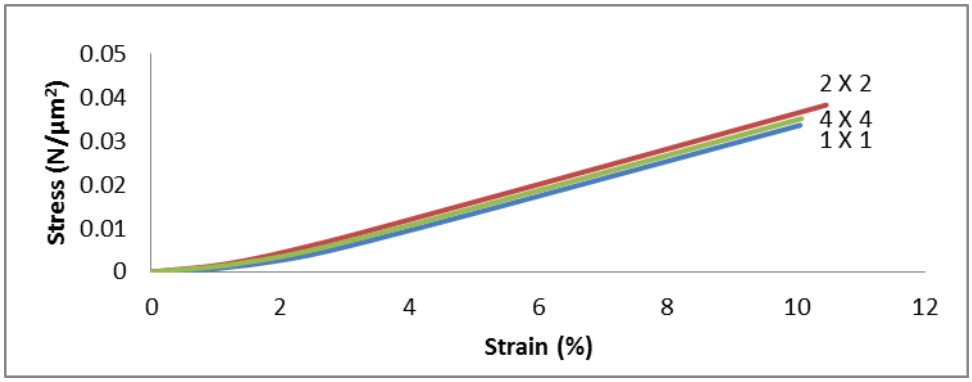

Fig 4.10 : (a) 1 x 1 RVE subjected to a specified displacement (b) 2 x 2 RVE subjected to a specified displacement (c) 4 x 4 RVE subjected to a specified displacement (d) Stress v/s Strain graph of Actin topology 1 for a specified displacement in y – direction.

In the above figure, although it is not showing a monotonic convergence, if we look at the difference between 1 x 1 and 2 x 2 RVE's, and 2 x 2 and 4 x 4 RVE's we can see that the difference is almost halved. Hence it can be inferred that the graph is converging.

4.2.2.2 Actin topology 2

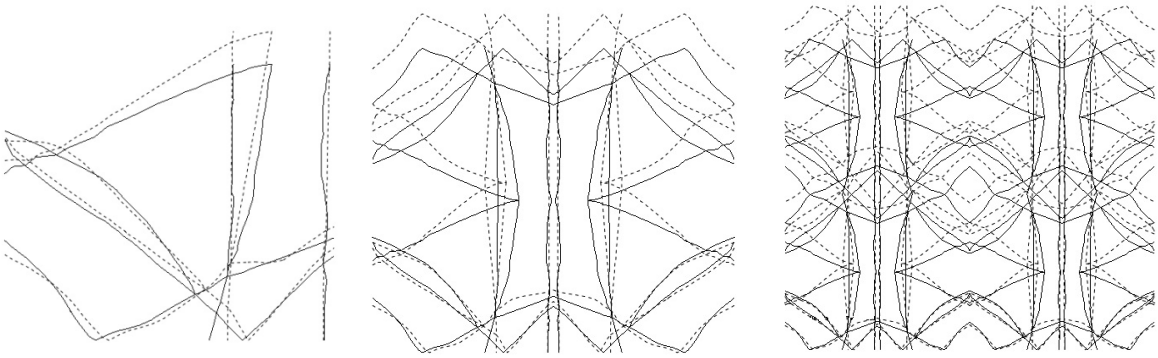

(a) (b) (c)

(d)

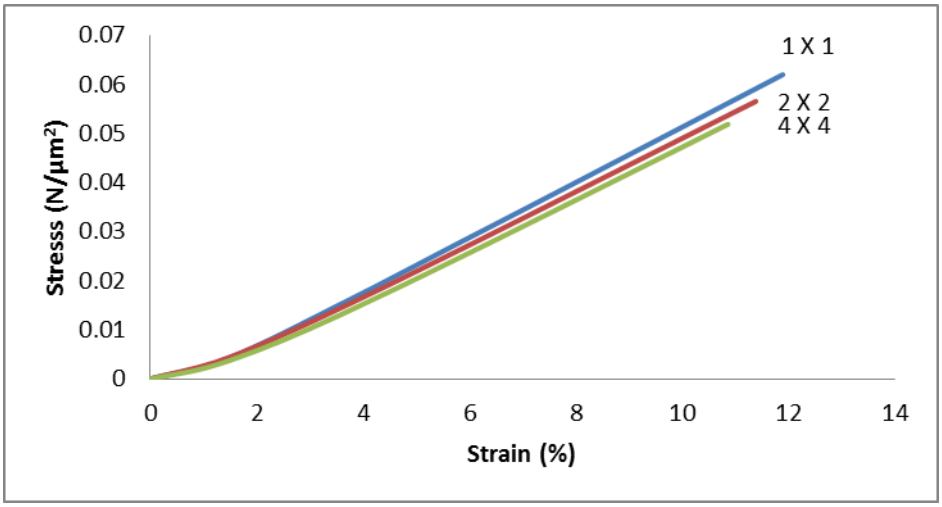

Fig 4.11 : (a) 1 x 1 RVE subjected to a specified displacement (b) 2 x 2 RVE subjected to a specified displacement (c) 4 x 4 RVE subjected to a specified displacement (d) Stress v/s Strain graph of Actin topology 2 for a specified displacement in y – direction.

The above graph shows a monotonic convergence. As we move from 1 x 1 to a 4 x4 RVE the differences are reduced as can be seen from the above graph. Hence it is a clear indication of a monotonic convergence.

4.2.2.3 Actin topology 3

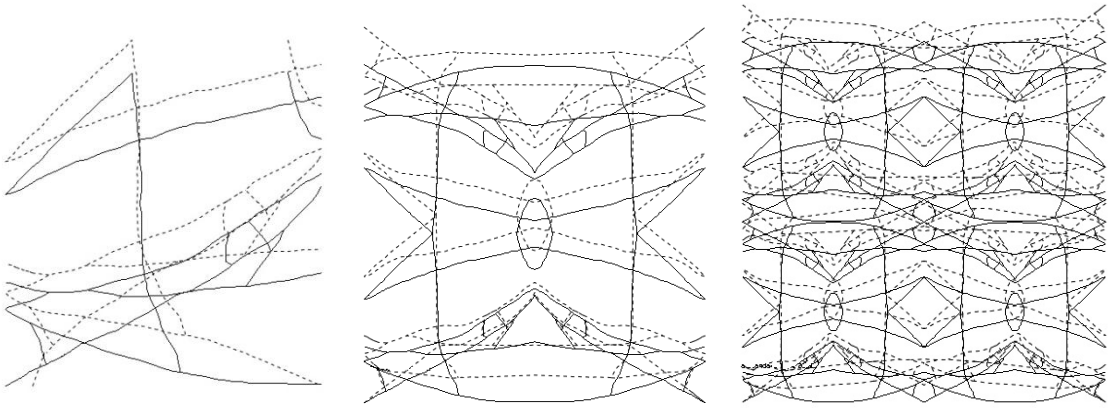

(a) (b) (c)

(d)

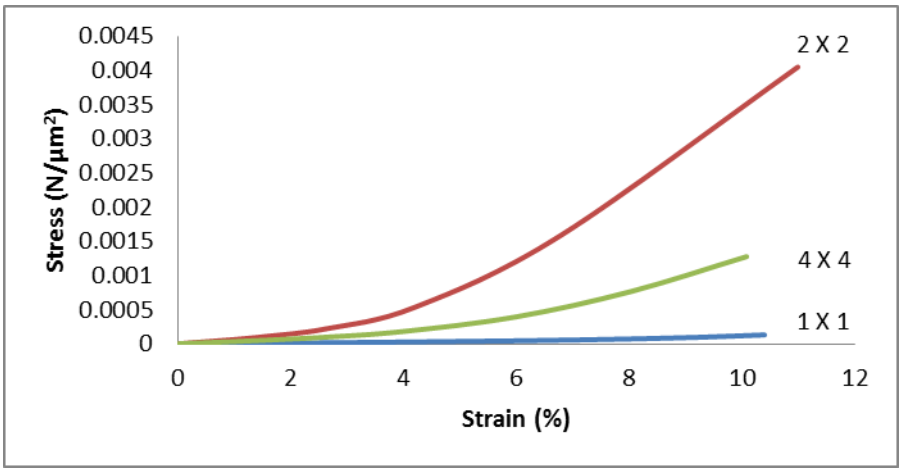

Fig 4.12 : (a) 1 x 1 RVE subjected to a specified displacement (b) 2 x 2 RVE subjected to a specified displacement (c) 4 x 4 RVE subjected to a specified displacement (d) Stress v/s Strain graph of Actin topology 3 for a specified displacement in y – direction.

The above graph shows large variation in stress for a specified displacement. The possible reason for it could be the unavailability of fixity at the bottom as can be seen from fig 4.12 and also the lack of available points to apply the specified displacement as only 2 nodes are available at the bottom to give fixity in all the three cases and only 2 points available at top for imparting the specified displacement.

4.3 Comparison of Actin topologies

All the three actin topologies were compared with each other using their respective 4 x 4 RVE's. The comparisons were made by finding out the behavior of the three topologies for the following three cases :

1. Specified displacement in x—direction
2. Specified displacement in y—direction
3. Specified shear deformation

4.3.1 Specified displacement in x—direction

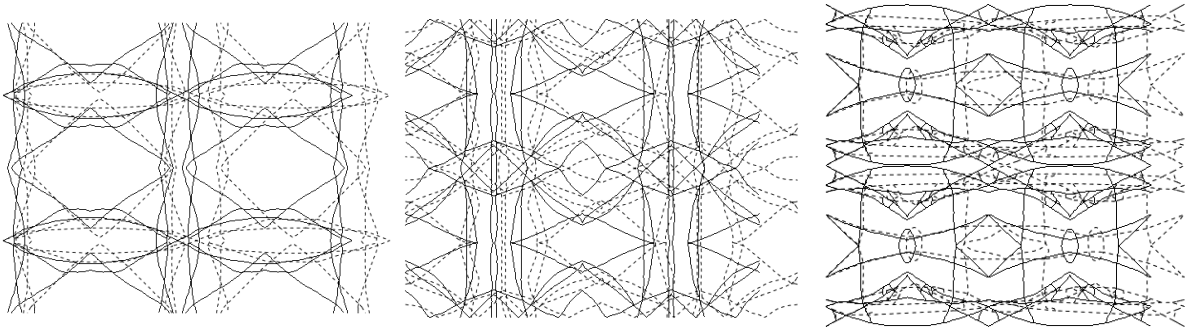

(a) (b) (c)

(d)

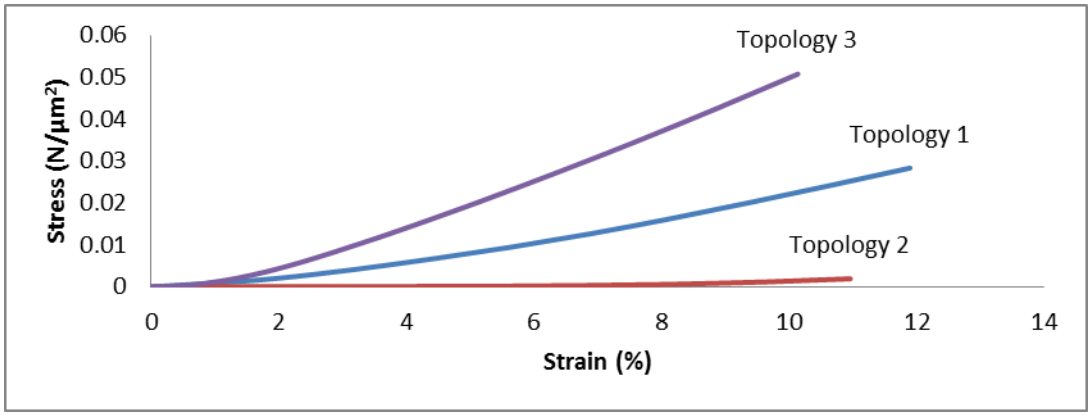

Fig 4.13 : (a) 4 x 4 RVE of Actin topology 1 (b) 4 x 4 RVE of Actin topology 2 (c) 4 x 4 RVE of Actin topology 3 (d) Stress v/s Strain graph of Actin topologies for a specified displacement in x-direction

The above graph shows that the topology 3 shows the largest response followed by topology 1 and topology 2. This behavior can be attributed to the orientation of these topologies and as the actin topology 3 is predominantly oriented towards x, it will undergo the least amount of bending (reorientation) before it starts taking the load. This behavior is also compliant with the characterization of different topologies given in Table 4.1.

4.3.2 Specified displacement in y—direction

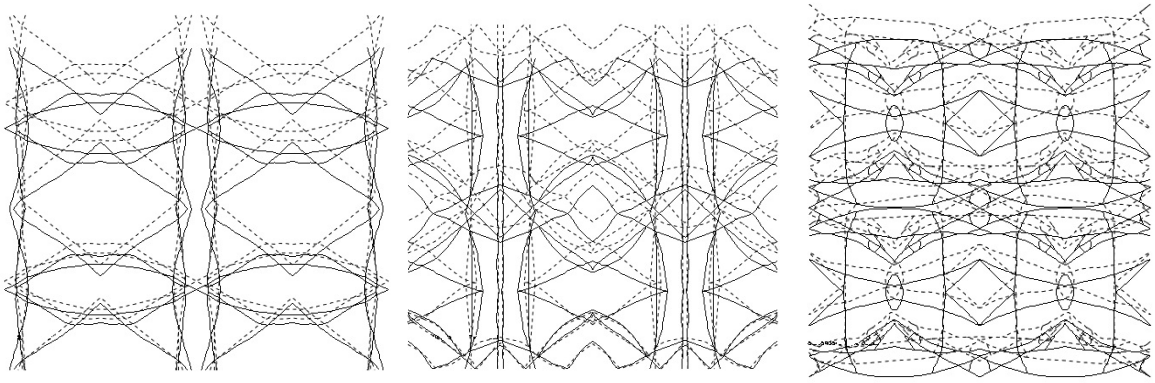

(a) (b) (c)

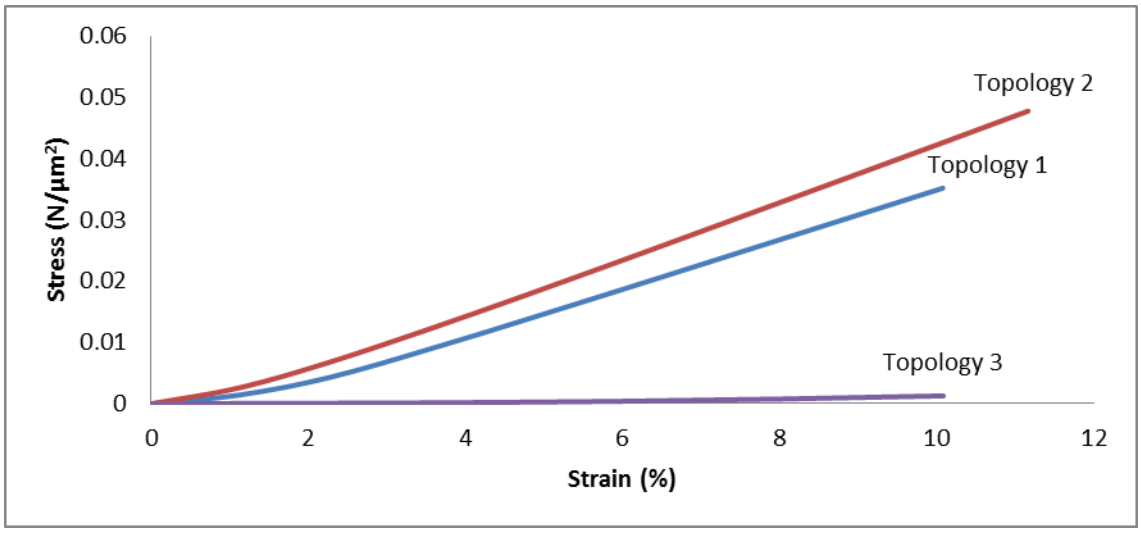

(d)

Fig 4.14 : (a) 4 x 4 RVE of Actin topology 1 (b) 4 x 4 RVE of Actin topology 2 (c) 4 x 4 RVE of Actin topology 3 (d) Stress v/s Strain graph of Actin topologies for a specified displacement in y-direction

It can be seen from the above figure that the actin topology 2 shows the largest response followed by actin topology 1 and actin topology 3. As the actin topology 2 is oriented predominantly in y direction as compared to the others, it will undergo the least amount of bending (reorientation) before it starts taking the load and hence the largest response. This is also in accordance with the characterization of different topologies given in Table 4.1.

4.3.3 Specified shear deformation

The 4 x 4 RVE's of the three actin topologies were compared by putting them through a specified shear deformation and finding out their respective response towards the specified shear deformation.

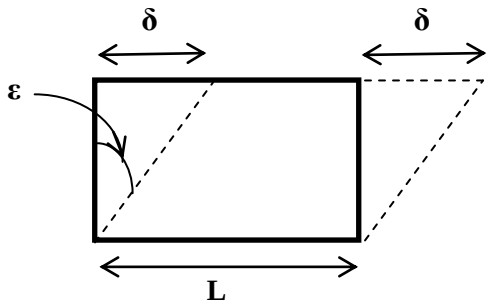

Fig 4.15 : Schematic diagram showing specified shear deformation.

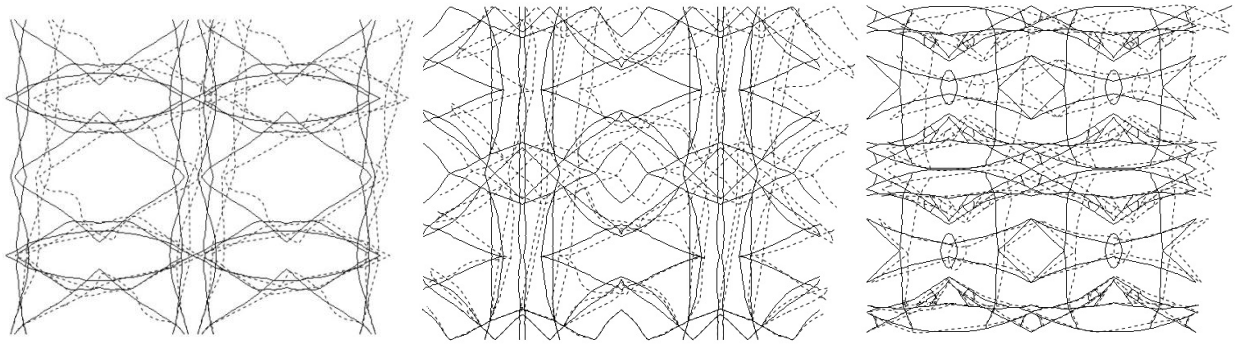

(a) (b) (c)

(d)

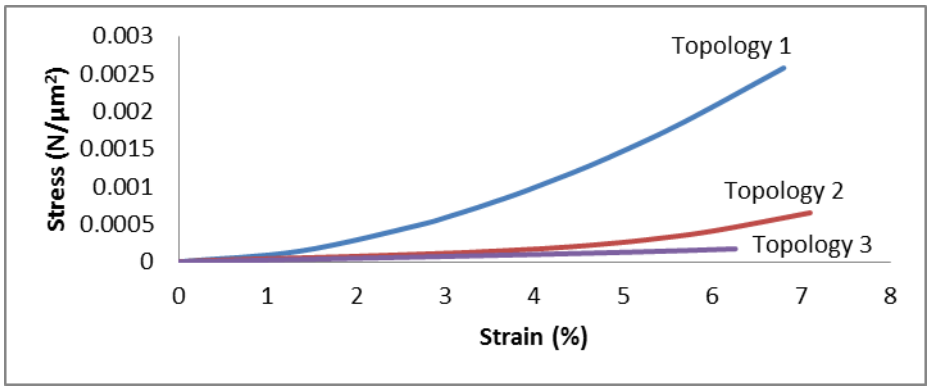

Fig 4.16 : (a) 4 x 4 RVE of Actin topology 1 (b) 4 x 4 RVE of Actin topology 2 (c) 4 x 4 RVE of Actin topology 3 (d) Stress v/s Strain graph of Actin topologies for a specified shear deformation

The above graphs show the behavior of different topologies in accordance with the characterization of different topologies given in Table 4.1 i.e., actin topology 1 is the most predominant in shear followed by actin topology 2 and actin topology 3 as almost equal amount of vertical as well as horizontal filaments are present in actin topology 1.

CHAPTER 5 MODELLING THE ACTIN CYTOSKELETON AND CELL MOTILITY

The basic structural elements of most cells is usually the same : fluid sheets enclose the cell and its compartments, while networks of filaments maintain the cell's shape and help organize its contents (Boal, 2002). The fluid sheets that enclose the cells are basically the cell membrane and the network of filament that maintain the cell's shape and help organize its contents are the actin filaments. In this chapter, we have tried to model a cell using only these two components neglecting all the other components of the cell as the major role with respect to the mechanical properties of the cell is played by the actin filaments. This cell is then put through a varying thermal field and an attempt is made to predict the motility of the cell.

5.1 Modelling the Actin cytoskeleton

5.1.1 Step 1 : Tiling

An average cell is usually about 10μm in diameter whereas the average size of the unit cell of all the three topologies in consideration is about 1.2 μm x 1.2 μm. Hence to model a complete cell out of the unit cell we tiled the mirror images of the unit cell 8 to 10 times in each direction depending upon their respective dimension in that axis to get to the required size. The tiling operation can be explained as follows :

For a given mesh M, we define three other meshes as follows:

1. H is M horizontally flipped
2. V is M vertically flipped
3. R is M both horizontally and vertically flipped

Using these four meshes as cells to build a lattice as follows, we can obtain a lattice of arbitrary size:

M	H	M	H	M	H
V	R	V	R	V	R
M	H	M	H	M	H
V	R	V	R	V	R

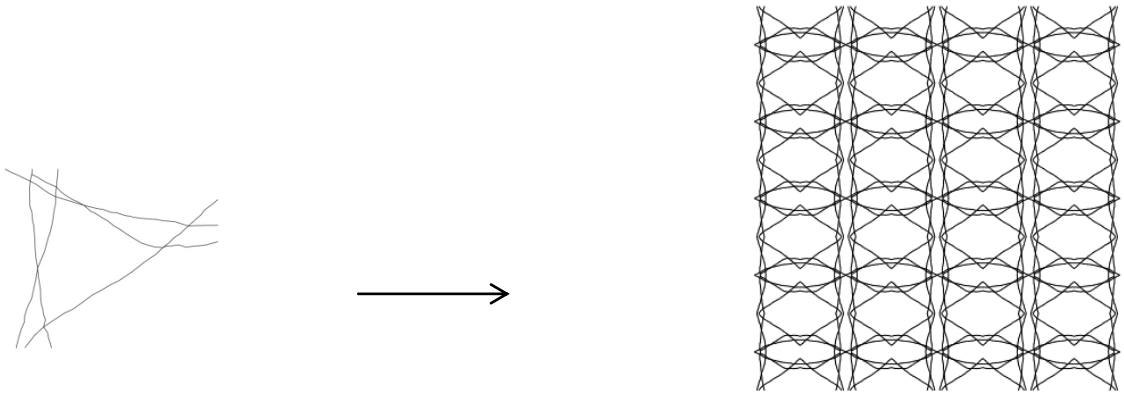

Fig 5.1 : 1 X 1 RVE is tiled using mirror images to 8 X 10 RVE

5.1.2 Step 2 : Cutting a circle

The tiling operation creates a rectangular mesh of size slightly above 10µm in each direction. An average cell is usually idealized as a circle with 10µm diameter whereas the mesh created by tiling yields a rectangle of dimensions slightly above 10µm. Hence to achieve a circular shape, the center of the mesh is found out and a circle of diameter 10µm is cut from this rectangle as shown in the figure below.

This step discards all nodes and elements of the mesh that fall outside the specified circular region. For each line segment, the part external to the circular region is determined, external points are deleted and the intersection point(s) of the line segment and the circle become an end-point of the line segment.

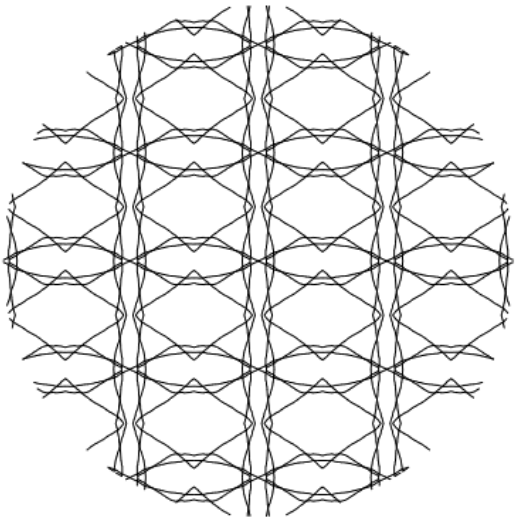

Fig 5.2 : The 8 X 10 RVE is cut into a circle of diameter 10µm

5.1.3 : Step 3 : Creating anchor points

To give the cell anchor points, the base was horizontally cropped at distance of 2µm from the bottom of the cell and the elements below that are omitted. This was done so that the base could be given the required fixity.

This step discards all nodes and elements of the mesh that fall below the specified horizontal line. For each line segment, the part above the crop line is determined, external points are deleted and the intersection point(s) of the line segment and the crop line become an end-point of the line segment.

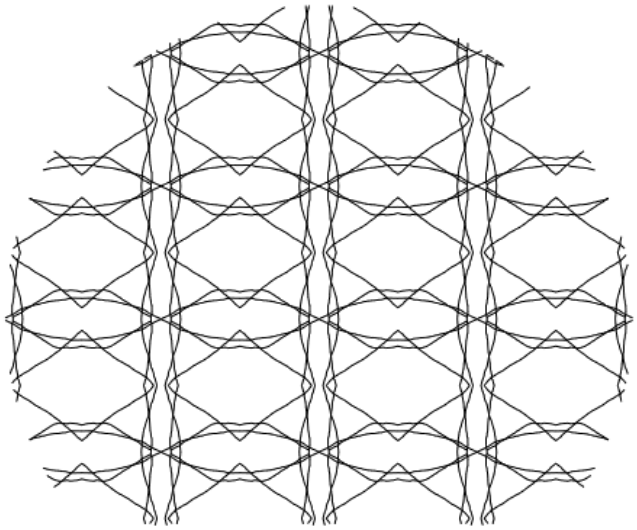

Fig 5.3 : The circle of diameter 10µm is cropped at distance of 2µm from the bottom of the cell and the elements below that are omitted.

5.1.4 Step 4 : Adding a cell membrane

In the last step, the only thing that remained was to add a membrane around the cell to give it a complete shape. This was done by adding a convex hull to the network shown in fig 5.3. The final shape of the cell created is shown in the figure below.

The **convex hull** of a finite set of points $S = \{P\}$ is the smallest polygon W that contains S.

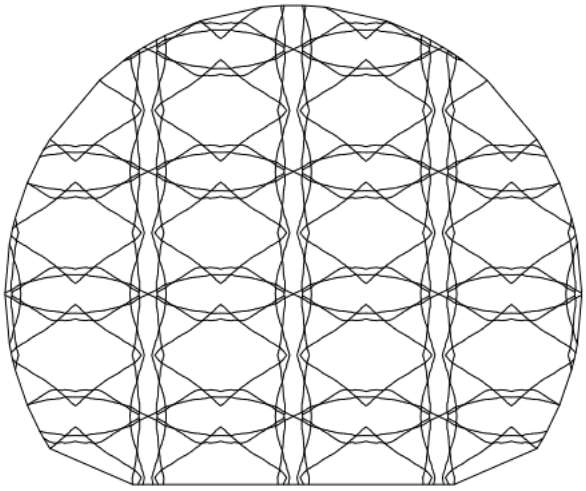

Fig 5.4 : A membrane is added around the cell.

5.2 Modelling cell motility

Cell motility is an essential element of numerous physiological processes in multi-cellular organisms, including wound healing, embryonic development, and cancer metastasis. (Bray 2001).

A well-described example of migrating cells is that of fibroblasts moving in a random or (semi)directional fashion over a two-dimensional surface, a migratory mode that is termed mesemchymal (Fig. 5.5).

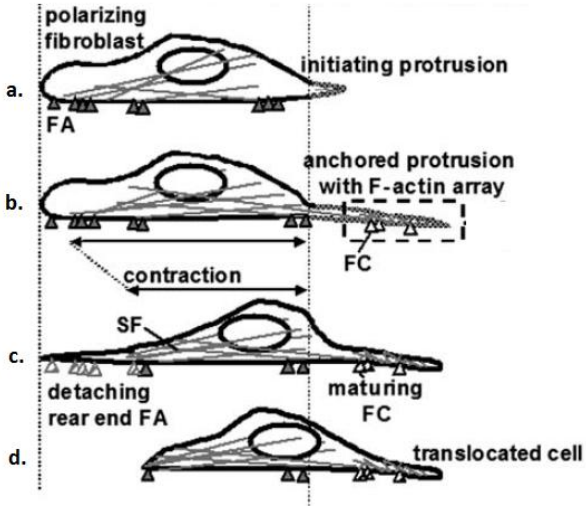

Fig 5.5 Cell migration is dependent on actin organization and dynamics. (a) protrusions form (b) anchoring via integrin based and actin array-associated focal contacts (FC) (c) contraction of stress fibers (SF) pulls the cell body forward, (d) rear end focal adhesion sites (FA) release. (Troys et al., 2008)

The cells succeed in moving or sliding in the "chosen" direction by repeating a four-step process as shown in fig 5.5.The process consists of (1) membrane protrusion at the front of the cell, (2) substrate adhesion of this leading edge, (3) cell body contraction, and (4) detachment of the rear end of the cell (Lauffenburger and Horwitz 1996; Mitchison and Cramer 1996). It is widely accepted and well documented that the actin cytoskeleton constitutes essential driving forces during all steps of this process (Lambrechts et al., 2004).

After the shape of the cell is created as in fig 5.4, the base of the cell was fixed and the cell was subjected to a predefined thermal field. This field was given increasing values. The progression of the cell towards the increasing thermal field is shown in fig 5.6 (a) to (e).

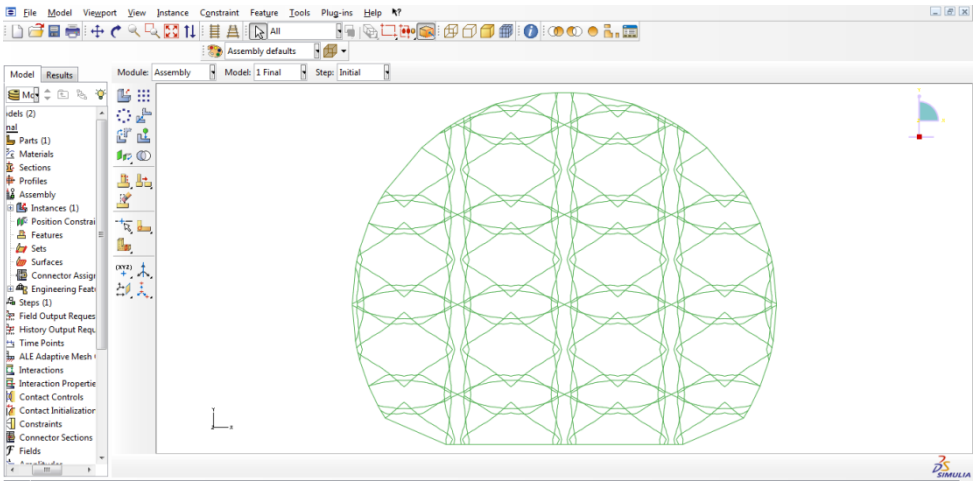

Fig 5.6 (a) : Initial cell shape before it is subjected to any specified strain

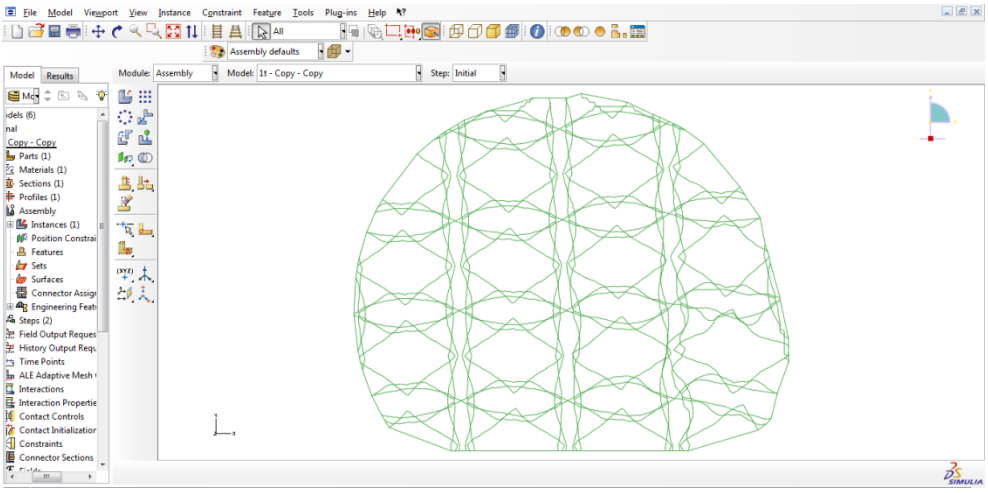

Fig 5.6 (b) : Cell shape after first increment in thermal field

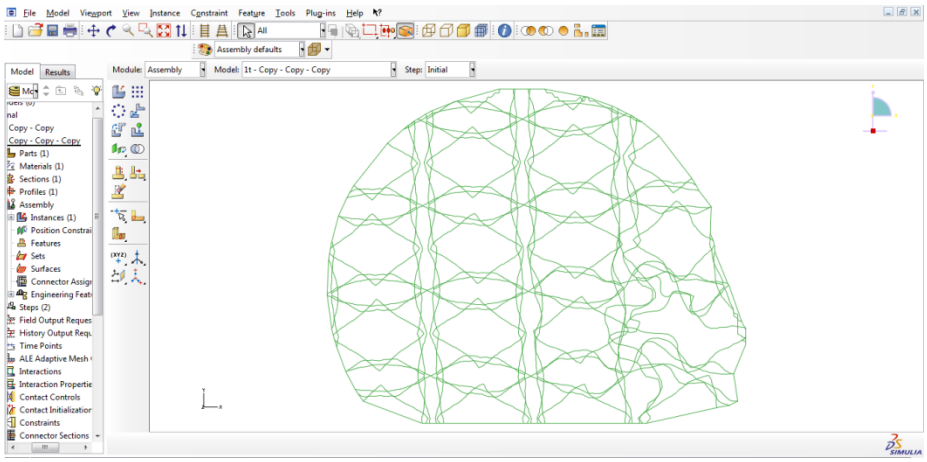

Fig 5.6 (c) : Cell shape after second increment in thermal field

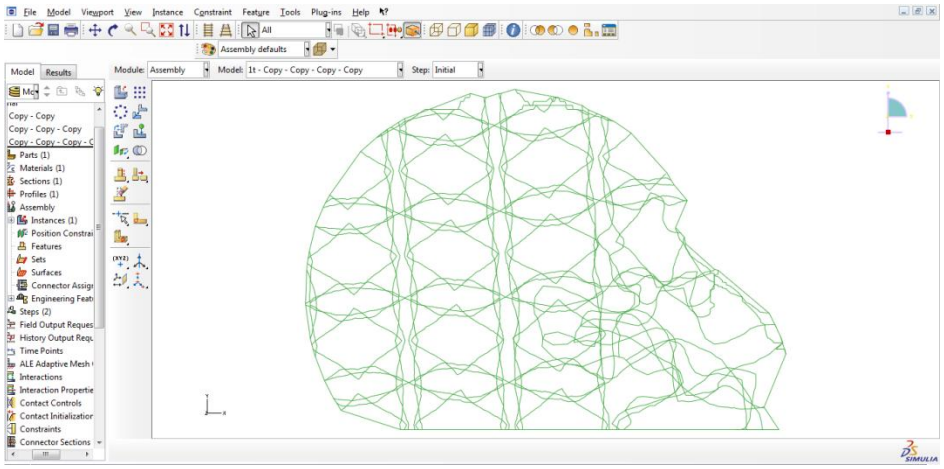

Fig 5.6 (d) : Cell shape after third increment in thermal field

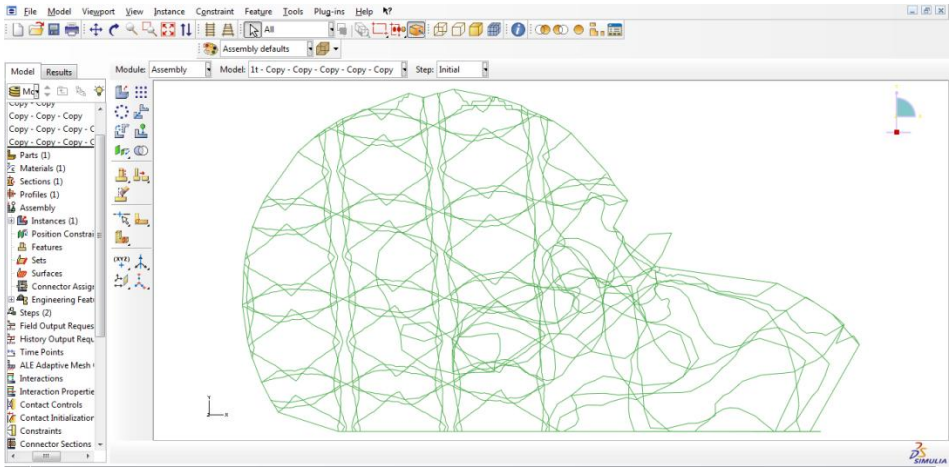

Fig 5.6 (e) : Cell shape after fourth increment in thermal field

As can be seen from the above figure, certain filaments are projecting out of the cell membrane. This is because the cell membrane properties have not being incorporated in this model. Further work needs to be done to incorporate the effects of the cell membrane into the model. Also the thermal field has not been characterized in this work and remains a gap to be filled.

As far as the modelling of the motility of cells is concerned, more work is required as this report only shows the membrane protrusion at the front of the cell. To complete a cycle of cell motility one must represent (1) membrane protrusion at the front of the cell, (2) substrate adhesion of the leading edge, (3) cell body contraction, and (4) detachment of the rear end of the cell.

CHAPTER 6 CONCLUSION AND FUTURE WORK

- Our work aimed to establish a framework to develop actin network geometries from a simple electron micrograph.
- Raster-vector transformations gave satisfactory results and hence the same procedure was adopted throughout this report.
- Out of the two filters used in vector refinement, the Proximity filter is the most effective.
- The characterization of actin topologies reveals that the three actin topologies are very different from each other. Based on the direction cosines we can deduce that

    a) In Actin topology 1, we can see that the difference in the values of the direction cosines is very less. This would result in an overall structure that would be predominantly a shear case.
    b) In Actin topology 2, the difference is higher and β has a high value. This would result in an overall structure that is predominant in y.
    c) In Actin topology 3, the difference is the highest and the value of α is much larger value. This would result in an overall structure that is predominant in x.

- Except for 2 cases, the topologies show a good convergent behavior.

- A couple of topologies show divergence i.e., Actin topology 2 in x direction and Actin topology 3 in y direction. For the first case, the possible reason for it could be the lack of points on the right edge to pull the network from. As can be seen from the fig 4.3 (a), on the right edge there are only 2 closely spaced points available to apply the specified displacement. For the second case, the possible reason for it could be the unavailability of fixity at the bottom as can be seen from fig 4.9 (a) and also the lack of available points to apply the specified displacement, only 2 points are available at the top for imparting the specified displacement.

- The comparison of topologies reveals that the behavior of the topologies is compliant with the characteristics deduced from the direction cosines.

- A whole cell actin cytoskeleton has been modelled and an attempt has been made to describe cell's motility in terms of varying thermal field.

- Extending the work to add more actin topologies to get a better hold on the mechanics of the actin cytoskeleton and the cell as a whole.
- Adding the appropriate properties to the cell membrane and getting a more realistic response of the cell.
- Characterization of the thermal field to create a better model of the cell's motility.
- Extending the work to 3-D since these are after all structures in 3-D space only.

CHAPTER 7 REFERENCES

Boal, D., 2002, Mechanics of the Cell, Cambridge University Press, New York.

Bray D, Cell Movements: From Molecules to Motility, second ed., Garland Publishing, New York, 2001.

Bruce Alberts, Molecular biology of the cell by, fourth edition, Garland science textbook, 2002

Cooper M Geoffrey, 2000, The cell : A Molecular Approach, 2nd edition, Sinauer Associates Inc., Sunderland.

Doi and Edwards, The Theory of Polymer Dynamics, 1999

Elson, E.L., 1988. Cellular mechanics as an indicator of cytoskeletal structure and function. Annu. Rev. Biophys. Biophys. Chem. 17, 397–430

Essential cell biology, 2003, 3rd edition, Garland science, Taylor and Francis group

Gardel M L, Shin J H, MacKintosh F C, Mahadevan L, Matsudaira P, Weitz D A, Elastic Behavior of Cross-Linked and Bundled Actin Networks, SCIENCE Vol. 304 28 May 2004

Haga, H., Sasaki, S., Kawabata, K., Ito, E., Ushiki, T., Sambongi, T, 2000. Elasticity mapping of living fibroblasts by AFM and immunofluorescence observation of the cytoskeleton. Ultramicroscopy 82 (1–4), 253–258

Head, D A, Levine A J, and MacKintosh F C, Phys. Rev. Lett. 91, 108102 (2003)

Head D A, MacKintosh F C, and Levine A J, Phys. Rev. E 68, 061907 (2003)

Hesketh, J.E., Prym, I.F. (Eds.), 1995. The Cytoskeleton . JAI Press, Greenwich.

Holmes K. C., Popp, D., Gebhard, W. & Kabsch, W. Nature, 347, 44-49. (1990).

Howard, J., 2001. Mechanics of Motor Proteins and the Cytoskeleton . Sinauer Associates Inc., Sunderland.

http://people.eku.edu/ritchisong/RITCHISO/301notes1.htm

http://www.wikipedia.org

Kreis T, Vale R, Cytoskeletal and Motor Proteins (Oxford Univ. Press, Oxford, ed. 2, 1999)

Kojima H, Ishijima A and Yanagida T, (1994), Direct measurement of stiffness of single actin filaments with and without tropomyosin by in vitro nanomanipulation, *Proc Natl Acad Sci U S A.* 91, 12962-6.

Lambrechts, A., Van Troys, M. and Ampe, C. 2004. The actin cytoskeleton in normal and pathological cell motility. Int. J. Biochem. Cell Biol. 6, 1890–1909.

Lauffenburger, D. A. and Horwitz, A. F. 1996. Cell migration: A physically integrated molecular process. Cell 84, 359–369.

Levine A J, The mechanics of semiflexible networks : Implications for the cytoskeleton, (2005)

Lodish et al., Molecular Cell Biology (Freeman, New York, ed. 4, 1999)

MacKintosh F C, Kas J, and Janmey P A, Phys. Rev. Lett. 75, 4425-4428 (1995)

Mitchison, T. J. and Cramer, L. P. 1996. Actin-based cell motility and cell locomotion. Cell 84, 371–379.

Onck P R, Koeman T, T. van Dillen, and E. van der Giessen, Phys. Rev. Lett. 95, 178102 (2005)

Paz M, Structural dynamics – Theory and computation (2004)

Rakoczy G A, Wawro Barbara and Gołaszewska S H, 2009, New Aspects of the Spontaneous Polymerization of Actin in the Presence of Salts

Rotsch, C., Radmacher, M., 2000. Drug induced changes of cytoskeletal structure and mechanics in fibroblasts: an atomic force microscopy study. Biophys. J. 78, 520–535

Sato, M., Theret, D.P., Wheeler, L.T., Ohshima, N., Nerem, R.M., 1990, Application of the micropipette technique to the measurement of cultured porcine aortic endothelial cell viscoelastic properties, J. Biomech. Eng. 112, 263–268

Storm C, Pastore J J, MacKintosh F C, Lubensky T C, and Janmey P A, Nature (London) 435, 191 (2005).

Stossel, T.P., 1984. Contribution of actin to the structure of the cytoplasmic matrix. J. Cell Biol. 99 (1), 15s–21s

Troys M V, Vandekerckhove J, and Ampe C, Actin and Actin-Binding Proteins in Cancer Progression and Metastasis, Protein Reviews, 2008, Volume 8, III, 229-277, DOI: 10.1007/978-0-387-71749-4_10

Tseng, Y., Wirtz, D., 2001. Mechanics and multiple-particle tracking microheterogeneity of alpha-actinin-cross-linked actin filament networks, Biophys. J. 81 (3), 1643–1656

Wang, N., 1998. Mechanical interactions among cytoskeletal filaments, Hypertension 32, 162–165

Yamazaki D, Kurisu S and Takenawa T, Regulation of cancer cell motility through actin reorganization, Cancer Sci vol. 96 no. 7 385 July 2005, doi: 10.1111/j.1349-7006.2005.00062.x